NATIONAL AERONAUTICS AND SPACE ADMINISTRATION

(NASA-CR-141847) RESULTS OF WIND TUNNEL RCS INTERACTION TESTS ON A 0.010-SCALE SPACE SHUTTLE ORBITER MODEL (51-O) IN THE CALSPAN CORPORATION 48-INCH HYPERSONIC SHOCK TUNNEL (TEST 0A93) (Chrysler Corp.) 115 p

N77-10132
HC A06
MF A01
Unclas
G3/16 08936

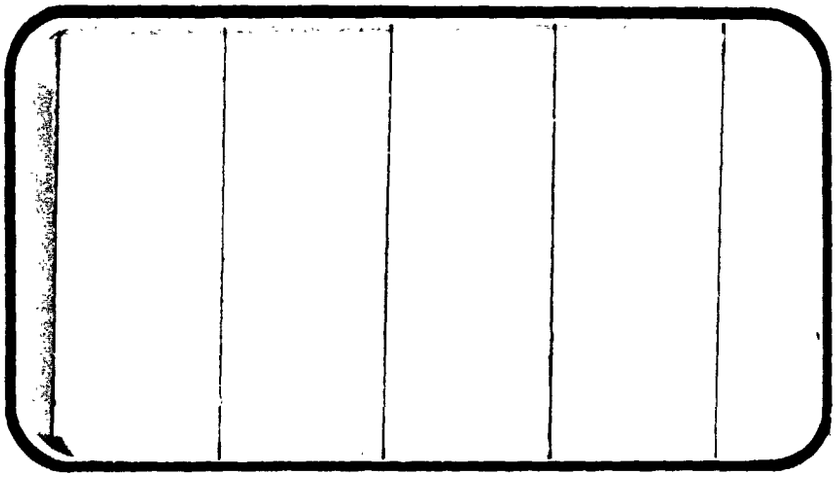

SPACE SHUTTLE

AEROTHERMODYNAMIC DATA REPORT

JOHNSON SPACE CENTER

HOUSTON, TEXAS

DATA MANagement services
SPACE DIVISION CHRYSLER CORPORATION

October, 1976

DMS-DR-2238
NASA CR-141,847

RESULTS OF WIND TUNNEL RCS INTERACTION TESTS ON A 0.010-SCALE SPACE SHUTTLE ORBITER MODEL (51-O) IN THE CALSPAN CORPORATION 48-INCH HYPERSONIC SHOCK TUNNEL (TEST OA93)

by

J. J. Daileda and J. Marroquin
Shuttle Aero/Sciences
Rockwell International Space Division

C. E. Rogers
Calspan Corporation

Prepared under NASA Contract Number NAS9-13247

by

Data Management Services
Chrysler Corporation Space Division
New Orleans, La. 70189

for

Engineering Analysis Division

Johnson Space Center
National Aeronautics and Space Administration
Houston, Texas

WIND TUNNEL TEST SPECIFICS:

Test Number:	Calspan 48-inch HST I84-120
NASA Series Number:	OA93
Model Number:	51-0
Test Dates:	October 28 through November 22, 1974
Occupancy Hours:	152

FACILITY COORDINATOR:

K. C. Hendershot
Calspan Corporation
P. O. Box 235
Buffalo, N. Y. 14221

Phone: (716) 632-7500

PROJECT ENGINEERS:

J. J. Daileda
J. Marroquin
Rockwell International
Space Division
12214 Lakewood Blvd.
Mail Code AD38
Downey, Ca. 90241

Phone: (213) 922-3785

C. E. Rogers
Brian Sheen
Calspan Corporation
P. O. Box 235
D/89
Buffalo, N. Y. 14221

Phone: (716) 632-7500
Ext. 8504

P. M. Schwartz
Rockwell International
Space Division
12214 Lakewood Blvd.
Mail Code AC07
Downey, California 90241

Phone: (213) 922-4843

DATA MANAGEMENT SERVICES:

Prepared by: Liaison--D. A. Sarver
Operations--D. B. Watson

Reviewed by: G. G. McDonald

Approved: _____
J. L. Glynn, Manager
Data Operations

Concurrence: _____
N. D. Kemp, Manager
Data Management Services

Chrysler Corporation Space Division assumes no responsibility for the data presented other than display characteristics.

RESULTS OF WIND TUNNEL RCS INTERACTION TESTS ON A 0.010-SCALE SPACE SHUTTLE ORBITER MODEL (51-O) IN THE CALSPAN CORPORATION 48-INCH HYPERSONIC SHOCK TUNNEL (TEST OA93)

by

J. J. Daileda and J. Marroquin
Shuttle Aero/Sciences
Rockwell International Space Division

C. E. Rogers
Calspan Corporation

ABSTRACT

An experimental investigation was performed in the Calspan Corporation Hypersonic Shock Tunnel (48-inch Leg) using an 0.010-scale SSV Orbiter Configuration 140A/B Model (51-O) to determine the effects of RCS jet/flow field interactions on SSV aerodynamic stability and control characteristics at various hypersonic Mach numbers and Reynolds numbers. Flow field interaction data were obtained using pitch and roll jets at Mach numbers of 10 and 20 at a unit Reynolds number of 0.85×10^5 per foot and at a Mach number of 10 at a unit Reynolds number of 6.1×10^5 per foot. In addition, direct impingement data were obtained at a Mach number of zero with the test section pumped down to below 10 microns of mercury pressure.

TABLE OF CONTENTS

INDEX OF FIGURES

INDEX OF FIGURES (Continued)

INDEX OF FIGURES (Continued)

INDEX OF FIGURES (Concluded)

INTRODUCTION

A 0.010-scale model of the Rockwell International Space Shuttle Vehicle Orbiter (Configuration 140A/B) was tested in the Calspan Corporation Hypersonic Shock Tunnel (48-inch Leg). Test dates were from Oct. 28, 1974 through Nov. 22, 1974.

The objective of the test was to determine the effects of RCS jet/flow field interaction on SSV aerodynamic stability and control characteristics at various hypersonic Mach numbers and Reynolds numbers.

Data were obtained for pitch and roll jets at Mach numbers of 10 and 20 at a unit Reynolds number of 0.85×10^5 per foot, and at a Mach number of 10 at a unit Reynolds number of 6.1×10^5 per foot. Direct impingement data were obtained at a Mach number of zero with the test section pumped down to less than 10 microns of mercury pressure.

All control surfaces (elevons, body flap, speed brake, and rudder) were set at zero deflection and an angle of attack of 30 degrees was set for the entire test. Some of the model photographs in this report show control surface deflections that are not zero, but all testing was conducted at zero control surface settings. Yaw and roll attitudes were set at zero for the entire test.

Data were obtained with RCS chamber pressure settings of 0 psi simulating RCS off, and 170, 680, and 1540 psi, which match the model RCS jet to tunnel free stream parameters of thrust ratio, momentum ratio, and plume shape for the three test conditions to the q = 5 psf full-scale free flight parameters. (See Table V).

NOMENCLATURE

SYMBOL	PLOT SYMBOL	DEFINITION
a		calibration constant, lb/mv or in-lb/mv
A		axial force, lbs.
b_w	BREF	wing span; lateral reference length, in
$\bar{c}$	LREF	wing MAC length, longitudinal reference length, in.
c_p		specific heat at constant pressure, ft-lbs/slug-°R
C_A	CA	axial force coefficient, $\frac{A}{q_\infty S_W}$
C_{cp}	C(CP)	cavity pressure coefficient, $\frac{P_{cav} - P_\infty}{q_\infty}$
C_ℓ	CBL	rolling moment coefficient, $\frac{\ell}{q_\ell b_w S_W}$
C_m	CLM	pitching moment coefficient, $\frac{m_c}{q_\infty S_W \bar{c}}$
C_N	CN	normal force coefficient, $\frac{N}{q_\infty S_W}$
C_n	CYN	yawing moment coefficient, $\frac{n_c}{q_\infty S_W b_w}$
C_p	CP	pressure coefficient, $\frac{P_m - P_\infty}{q_\infty}$
C_Y	CY	side force coefficient, $\frac{Y}{q_\infty S_W}$
C'_∞		(see Data Reduction Section)
C^*_∞	C*	(see Data Reduction Section
$\sqrt{C^*_\infty}$	SQRTC*	(see Data Reduction Section)

NOMENCLATURE (Continued)

SYMBOL	PLOT SYMBOL	DEFINITION
$\bar{h}$		vertical distance from balance center to model MRC, inches
H_o	H(O)	total enthalpy, ft-lbs/slug, H_o was multiplied by 10^{-6} for data display
H_w	H(W)	enthalpy at wall conditions, ft-lbs/slug, H_w was multiplied by 10^{-6} for data display
L/D		lift to drag ratio, CL/CD
ℓ		rolling moment about the balance center, in-lbs.
ℓ_b		Orbiter reference body length, inches
m		pitching moment about the balance center, in-lbs.
M_i	M(I)	incident shock Mach number
M_∞	MACH	Mach number
MRC	MRP	model moment reference center (X_o, Y_o, Z_o), in.
n		yawing moment about the balance center, in-lbs.
N		normal force, lbs.
P		pressure, psia
Pc	PCRCS	RCS Plenum Chamber Pressure, Psia
P_{m_j}	PMj	pressure measured on model at tap number j = 1,2,3,4, psia
P_o	P(O)	stagnation pressure, psia
P'_o	PITOT	stagnation pressure behind a normal shock, psia
P_{TS}	P(TS)	pressure in the test section before a test, microns

NOMENCLATURE (Continued)

SYMBOL	PLOT SYMBOL	DEFINITION
P_∞	P	freestream static pressure, psia
q_∞	Q(PSI)	freestream dynamic pressure
$\bar{q}S/T$		inverse RCS thrust coefficient
R_e/ft	RN/L	Reynolds number per foot, $\frac{\rho_\infty U_\infty}{\mu_\infty}$, $\frac{1}{ft}$ Re/ft was multiplied by 10^{-6} for data display
Re_ℓ	REFTL	Reynolds number, $\frac{\rho_\infty U_\infty \ell_b}{\mu_\infty}$ Re was multiplied by 10^{-6} for data display
$S_{cav.}$		model reference cavity area, in.^{2}
S_W	SREF	model wing reference area, in^2
TH		RCS nozzle thrust, lb.
T		temperature, °R
T_0	T(0)	total temperature, °R
T_W	T(W)	temperature at wall conditions, °R
T'		(See Data Reduction Section)
T*	T*	(see Data Reduction Section)
T_∞	T	freestream static temperature, °R
$\bar{u}$		longitudinal distance between the balance center and the model MRC, inches
U_j		RCS nozzle exit gas velocity, ft/sec
U_∞	U	freestream velocity, ft. per sec.
$\bar{v}$		spanwise distance between the balance center and the model MRC, inches

NOMENCLATURE (Continued)

SYMBOL	PLOT SYMBOL	DEFINITION
$\bar{V}_\infty^*$	VBAR	(see Data Reduction section)
$\bar{V}_\infty'$	VLBAR	(see Data Reduction section)
X_{cp}/ℓ_b	XCP/L	normal force center of pressure, $0.65 - \frac{(C_m)}{CN}\frac{(\bar{c})}{\ell_b}$, percent model length
ν_i		ith component balance capsule output, i = 1,2,...6, mv
X_{MRC}	XMRP	longitudinal location of MRP, in. X_0 Orbiter longitudinal station, in.
X_0	XO	Orbiter longitudinal station, in.
Y		side force, lbs.
Y_{MRC}	YMRP	lateral location of MRP, in. Y_0
Y_0	YO	Orbiter lateral station, in.
Z_{MRC}	ZMRP	vertical location of MRP, in. Z_0
Z_0	ZO	Orbiter vertical station, in.
α	ALPHA	model angle-of-attack, degrees
γ		specific heat ratio
δ_{BF}	BDFLAP	body flap deflection, degrees
δ_e	ELEVON	elevon deflection $(\delta e_L + \delta e_R)/2$, degrees
δ_r	RUDDER	rudder defiection, degrees
δ_{SB}	SPDBRK	speedbrake deflection, degrees
μ_∞	MU	freestream absolute viscosity coefficient, slugs/ft-sec. μ_∞ was multiplied by 10^8 for data display
ρ_∞	RHO	freestream density, slugs/ft^3; ρ_∞ was multiplied by 10^6 for data display

NOMENCLATURE (Concluded)

SYMBOL	PLOT SYMBOL	DEFINITION
σ	SIGMA	standard deviation
ϕ	PHI	angle of roll, degrees
β	BETA	angle of sideslip, degrees

SUBSCRIPTS

1	driven gas initial conditions
4	denotes region behind reflected shock
AF	data based on tunnel airflow calibrations
c	corrected
cav.	cavity
cp	center of pressure
E	data based on estimated values for q_∞ (ref. 14)
i	incident shock in driven gas
L	left
m	model
0	nozzle supply stagnation conditions; Orbiter reference system
o′	stagnation conditions behind a normal shock
R	right
ref.	reference
W	wing reference; conditions at wall
∞	freestream conditions
j	static pressure tap number, RCS nozzle exit condition

REMARKS

Test Summary

Test 0A93 activity at the Calspan Hypersonic Shock Tunnel commenced on Oct. 28, 1974 and was completed Nov. 23, 1974. Installation of the sector, "E" nozzle, model, RCS system, and Schlieren system required six days; check-out of the balance in the tunnel took one day; check-out and modification of the RCS system took seven days; and testing was conducted for 5 days. A total of 152 hours of testing activity (equivalent to occupancy hours) were used to obtain 15 runs, eleven of which yielded data.

Precision of Data

Stagnation enthalpy and the test section free stream conditions were calculated using the thermodynamic properties of real air, the incident shock wave velocity, and the nozzle supply pressure. The speed of the incident shock wave was measured to within ±1 percent. Based on the agreement of pressure transducers, the nozzle supply pressure is considered accurate to within ±3.5 percent. Dynamic pressure was determined from a linear correlation of measured model pressures and forces (see Data Reduction section); therefore, one would expect the most probable error in dynamic pressure to reflect the accuracy of these measurements, which is ±5 percent and ±3 percent, respectively. The resultant most probable error in dynamic pressure is calculated as ±5.8 percent. The test section Mach number, which is in turn dependent upon the ratio of P_{0_2}/P_0 and q_∞/P_0, is then estimated to be accurate to ±2 percent.

REMARKS (Continued)

Model attitude was set with an inclinometer at the desired angles of pitch and roll, and are estimated to be within ±0.1 degree.

On the basis of calibration repeatability and on the consistency and the repeatability of the pressure data, it is estimated that these data have a "most probable error" of ±5 percent.

Uncertainties in force coefficients arise from errors in q_∞, reference area, and balance loads. The error in q_∞ is covered in the Data Reduction section. If one assumes a negligible error in the reference area, then all that is needed to obtain the overall accuracy of the force data is a knowledge of the precision of measuring the balance loads. On the balance output, there will be an incremental error based on the capability of the balance to read a given load. This type of uncertainty would put on the data plot a band which would be independent of angle of attack. These incremental errors are obtained by calculating the 3σ deviation between applied and calculated calibration loads. (For a normal or Gaussian distribution of errors, 1σ contains 68.3 percent of the data compared to 99.7 percent of the data for 3σ; therefore, 3σ is considered more applicable here.) The calculated loads were determined by using the calibration constants and the balance output data produced by the applied loads.

For the static calibrations used in the program, the results are as follows:

REMARKS (Concluded)

Component	3σ Deviation Value	Percent of Full-Scale
N	± .696 pound	0.7
m	±1.254 inch-pounds	2.1
Y	±2.325 pounds	3.7
n	±2.010 inch-pounds	4.7
ℓ	± .243 inch-pound	2.0
A	± .198 pound	0.5

CONFIGURATIONS INVESTIGATED

The model for these tests was a 0.010-scale replica of the Rockwell International Space Shuttle Vehicle Configuration 140A/B, designated Model 51-O. SSV Orbiter Configuration 140A/B is composed of the configuration control drawing VL70-000140A body and the VL70-000140B wing. A three-view drawing of the orbiter configuration is shown in figure 2a.

The metric orbiter components are constructed of AZ31B magnesium and consist of the following items: fuselage, wing, vertical tail, orbital maneuvering system (OMS) pods, simulated lower orbiter main engines, speed brake, and body flap. All control surfaces (elevons, body flap, rudder, and speed brake) remained in their undeflected positions for the entire test.

The aft end of the OMS pods have been modified to allow installation of simulated RCS nozzles. A plenum for supplying air to these nozzles is mounted at the rear of the orbiter fuselage, between the RCS nozzles. Two RCS nozzle blocks were used, each with 2 nozzles. RCS plenum and nozzle blocks are non-metric, and are clamped on the sting, aft of the model, with a gap of 0.30-inch between the metric OMS pods and non-metric RCS nozzle blocks. Figure 2b shows nozzle block geometry.

Nomenclature below were used to designate the orbiter model components. $O_1 = B_{26}\ C_9\ E_{26}\ F_7\ M_{15}\ N_{76}\ R_5\ V_8\ W_{116}$

(Non-metric RCS nozzle blocks are plenum-mounted at base of orbiter.)

$O_2 = O_1$ with non-metric RCS nozzle blocks, plenum, and supply pipe removed from base of orbiter.

CONFIGURATIONS INVESTIGATED (Concluded)

The orbiter components are defined as follows:

Symbol	Component	Configuration	Lines Drawing	Model Drawing
B_{26}	Body	140A/B	VL70-000140A VL70-000193	VF109558 (AEDC) VF109560 (AEDC) R80054 (Lockheed)
C_9	Canopy	3A	Same as B26	VF109558 (AEDC)
E_{26}	Elevon	140B	VL70-000140B VL70-000200	VF109559 (AEDC)
F_7	Body Flap	3A	VL70-000140A VL70-000145	VF109559 (AEDC) SSA01247 (AEDC)
M_{15}	OMS Pod	3A	VL70-000145	VF109561 (AEDC)
N_{76}	Lower Main Engines	3A	VL70-000140A VL70-005106A	SAA01247
R_5	Rudder	140A/B	VL70-000095	VF109559 (AEDC)
V_8	Vertical	3A	VL70-000140A	VF109559 (AEDC)
W_{116}	Wing	140B	VL70-000140B VL70-000200	VF104559 (AEDC) VF109560 (AEDC)

RCS nozzle blocks are defined as follows:

Symbol	Definition
N_{43}	Twin left side pitch down RCS nozzles sized to simulate the prototype 3A configuration (VL70-000140A) aft RCS pitch engines at q_∞ = 5 psf and M_∞ = 29.0 with a wind tunnel Mach number of 10.3. Nozzles are canted 12° aft and 20° outboard.
N_{44}	Twin right side pitch up RCS nozzles, sized the same as N43. Nozzles are not canted.

Model component dimensional data are given in table III. Reference 12 and 15 give additional model information.

INSTRUMENTATION

Force data were measured with the Calspan 1.312-inch diameter six component "E" balance. This balance is a piezoelectric balance using six lead zirconium titante ceramic load cells mounted to a non-metric platform, which is integral with the sting support. A sketch of the balance is shown in figure 2e. Accelerometers were installed in the model to form an acceleration balance which, when combined with the force balance, resulted in an internally compensated balance system. The accelerometer balance consists of six individual accelerometers (equal in number to the number of force and moment components) mounted individually within the model. Their locations and axes were selected for maximum imposed acceleration; i.e., at model extremities for pitch, roll, and yaw. An analog computer was used to combine signals from the balances, six force beams (3 normal, 2 side, and 1 axial) and the six accelerometers to yield internally compensated electrical outputs, directly proportional to the applied forces and moments.

A grounding (fouling) circuit was provided between the sting and the metric orbiter main propulsion engine nozzles.

The model cavity and pitot pressures were measured by a system developed to meet the particular requirements of shock tunnel testing. The pressure transducers employ piezoelectric crystals, and their small size permits installation within the model. The transducers used in this test have a dual-element feature which reduces acceleration effects to an indicated pressure of .0003 psi/g. Pressures as low as .0008 psi may be

accurately measured by these transducers. Proper shielding of the elements precludes temperature effects in the short test time.

Four locations on the bottom surface of the orbiter body and wing were instrumented with Calspan piezoelectric pressure transducers. These transducers are acceleration compensated and were located on the model as specified below.

PRESSURE X-DUCER NO.	PRESSURE COEFFICIENT NUMBER	LOCATION ORBITER COORDINATES, INCHES MODEL SCALE	
P_{m1}	CP1	LOWER WING SURFACE	X_o = 11.887 Y_o = 2.810
P_{m2}	CP2	LOWER WING GLOVE	X_o = 10.782 Y_o = 1.821
P_{m3}	CP3	LOWER FUSELAGE CENTERLINE (AFT)	X_o = 11.887 Y_o = 0.000
P_{m4}	CP4	LOWER FUSELAGE CENTERLINE (FORWARD)	X_o = 4.000 Y_o = 0.000

Figure 2c shows the pressure locations on the model.

Orbiter base pressure was not measured on this test. However, the balance cavity pressure was measured using a Calspan piezoelectric pressure transducer.

The RCS plenum chamber was instrumented to monitor plenum wall pressure. This pressure was measured using PCB Model 113M01 transducer supplied by Calspan.

INSTRUMENTATION (Concluded)

The Schlieren system used was of the double-pass collinated type with the knife edge horizontal. This system was used to provide the sensitivity needed to obtain photographs of shock waves during low density runs. Schlieren photographs were taken during most runs.

The outputs from the pressure transducers and the force-balance system were recorded on the magnetic drum of a Navigational Computer Corporation MCL-100 data acquisition system (NAVCOR), which samples the data from each of 48 channels every 50 microseconds. The data from the drum are transferred to a Brush recorder for immediate examination and preliminary calculations. The average voltages obtained from the Brush recorder were subsequently punched on cards for reduction on an IBM 370-168 computer.

TEST FACILITY DESCRIPTION

The basic components of the 48-inch Hypersonic Shock Tunnel (HST) are shown in figure 2d and described in reference 1. The tunnel employs a constant-area shock tube with an 8-inch inner diameter. The driver tube is 20 feet long and is externally heated by a resistance heater to temperatures of 1460°R. The driven tube is 50 feet long. The driver gas is generally a mixture of helium and nitrogen with a maximum helium purity of 100% while the driven gas is generally air. Steady-flow test times of duration sufficient to permit accurate measurement of the various parameters of interest are achieved with the tailored-interface technique. A basic discussion of shock tunnel operation technique can be found in reference 1.

Three axisymmetric nozzles are available to expand the test gas to high velocities:

Nozzle	Type	Exit Diameter in Inches	Test Section Mach Number
A	Contoured	24	5.5 to 8
D	Contoured	48	10 to 16
E	10½° Semi-angle cone	48	9 to 20

The "E" nozzle was used for this program to obtain the highest Mach number possible. The nozzles employ replaceable throat inserts of different diameters so that with the particular nozzle, the test Mach number can be varied. Test air passes downstream of the test section into a receiver tank of a size sufficient to maintain the desired flow for dura-

tions of 5 to 13 milliseconds. All nozzles have been calibrated using pitot-pressure survey rakes over the Mach number range indicated.

The test section is equipped with two 16-inch diameter Schlieren windows mounted a short distance aft of the nozzle exit.

TEST PROCEDURE

The force balance system was first statically calibrated by hanging a series of weights on the balance and recording the force capsule voltage outputs. The model was then mounted on the balance, and an inertial compensation procedure, in which the model underwent known translational and rotational accelerations about three chosen axes, was conducted. Resultant signals were used as inputs to an analog computer. By combining the force balance and accelerometer signals, the computer supplied as outputs to the recording system the values for the aerodynamic forces and moments. Once the balance was compensated, a dynamic check calibration was made of the complete model balance system to verify the accuracy of the compensation. This procedure consisted of rapidly releasing known loads from the model and recording six-component acceleration-compensated balance data.

Pressure transducers were calibrated (i.e., voltage output vs. applied pressure) after installation in the model. The voltage variation of the transducer is linear over the range of pressure normally encountered during testing. This calibration, in conjunction with estimated values for the model pressures to be experienced during the actual test, provided the basis for adjusting the gain of the data recording system to achieve maximum "readability". The detailed calibration data are kept on file at Calspan.

The RCS nozzle blocks used for this test were calibrated in the Rockwell International Rocketdyne Division Rocket Nozzle Test Facility

prior to the test. Procedures used for these calibrations are described in reference 13. Calibration curves of vacuum thrust versus chamber pressure are given in figure 4a.

The model was installed on the Calspan 1.312-inch diameter six-component "E" balance assembly supported by the Calspan 1-inch diameter H61-1042-5 sting. The sting was attached to the light load sector using vibration isolating pads.

A quick-acting solenoid-actuated Valcor valve was mounted on a bracket in proximity to the base of the model to supply high pressure air to the RCS system. The supply line for this valve was attached to a 10-inch diameter plenum tank mounted in the tunnel receiver tank, aft of the model. Prior to each RCS run, the tank was loaded to the RCS operating pressure from the Calspan high pressure air system. Plenum pressure was set with either a U.S. Gage 300 or 3000 psig gage, depending on the pressure level. During each RCS run, firing of the Valcor valve was synchronized with operation of the tunnel so that the peak RCS pressure coincided with the usable test time.

It was necessary to solve unexpected installation, instrumentation, and operational problems before usable data cound be obtained. Problems which were peculiar to plume simulation in a short duration run type of hypersonic facility are enumerated below:

1. The Valcor valve (for RCS operation) was moved from the sting to a bracket mounted on the floor, next to the sting. This isolated the

valve and plumbing from the sting-balance system, the only connection between the two being a flex line, and reduced the mechanical shock and electromagnetic interference effects of the balance caused by the valve.

2. Electronic filters were installed in the Navcor computer to eliminate the large noise signals caused by firing the Valcor valve.

3. Synchronization of RCS system peak pressure with tunnel run time was accomplished by fine-tuning the inputs into the delay generator in the Valcor valve firing system. Several check runs were made to determine the proper timing delay.

DATA REDUCTION

With the exception of q_∞ and P'_0, standard Calspan data reduction methods were used to compute force and moment coefficient data, center of pressure locations, and the remaining test section conditions. Reference 3 describes the Calspan standard data reduction methods used for the Hypersonic Shock Tunnel

From the model-balance system static calibration data, a matrix was computed that relates the applied loads and moments to the balance outputs, accounting for all interactions and the location of the specified moment reference center. Aerodynamic forces and moments were then computed from the matrix, which for the six component balance has the form:

$$\begin{Bmatrix} N \\ m \\ Y \\ n \\ \ell \\ A \end{Bmatrix} = a_{ij} \begin{Bmatrix} X_1 \\ X_2 \\ X_3 \\ X_4 \\ X_5 \\ X_6 \end{Bmatrix}$$

where X = balance capsule output in millivolts

a = calibration constant (lb/mv or in-lb/mv)

N = normal force, lbs.

m = pitching moment about the balance center, in-lbs.

A = axial force, lbs.

Y = side force, lbs.

ℓ = rolling moment about the balance center, in-lbs.

n = yawing moment about the balance center, in-lbs.

DATA REDUCTION (Continued)

In addition, the pitching, yawing and rolling moment coefficients about the model moment reference center and axial force corrected for model cavity pressure were computed from the following equations:

$$m_c = m + \bar{u}\, Y + \bar{h}\, A_c \qquad (1)$$

$$n_c = n + \bar{u}\, Y + \bar{v}\, A_c \qquad (2)$$

$$\ell_c = \ell + \bar{h}\, Y - \bar{v}\, N \qquad (3)$$

$$A_c = A + S_{cav.}\,(P_{cav.} - P_\infty) \qquad (4)$$

where:

$\bar{u}$ = -0.519 inch

$\bar{h}$ = +0.250 inch

$\bar{v}$ = 0.0 inch

$S_{cav.}$ = 4.5 in^2

The pressure transducers measure the difference between the initial test section pressure and the applied local pressure. The initial pressure is of the order of 5 microns and is added to the measured pressure to obtain the absolute model pressure. The local pressure coefficient C_p was then computed.

The test conditions of pressure, temperature and Reynolds number are computed by assuming isentropic expansion of the test gas from the conditions behind the reflected shock in the driven tube to the test section Mach number. The flow is expanded sufficiently so that the air in the test section is cool enough to obey the perfect gas laws.

The stagnation enthalpy and temperature of the air behind the reflected shock is determined from

$$H_o = H_1\,(H_4/H_1) \qquad (5)$$

and $$T_o = T_1\,(T_4/T_1), \text{ respectively} \qquad (6)$$

where H_4/H_1 and T_4/T_1 are functions of U_i, the incident shock velocity.

DATA REDUCTION (Continued)

(References 4-6). U_i is obtained by measuring the time taken by the shock wave to pass between two stations in the shock tube. H_1 is taken from reference 7. Free stream static temperature is obtained from

$$T_\infty = \frac{H_o}{C_p} \left(1 + \frac{\gamma - 1}{2} M_\infty^2\right)^{\gamma-1} \tag{7}$$

Free stream pressure is calculated using

$$P_\infty = P_p P_o \left[1 + \frac{\gamma-1}{2} M_\infty^2\right]^{\left(\frac{-\gamma}{\gamma-1}\right)}$$

where:

$$P_p = \left[\frac{(P/P_o)\text{real}}{(P/P_o)\text{perf.}}\right] \tag{8}$$

is the real gas correction to the ideal static-to-total pressure ratio as described in reference 8. The source data used in this technique are references 7 and 9.

Values for absolute viscosity (μ) used to compute Reynolds numbers were obtained from reference 10 for temperatures below 500°R.

Stagnation conditions behind a normal shock in the test section are based on the data of reference 9. The balance of the primary test section properties is based on perfect gas theory.

The normal procedure used to determine free-stream Mach number is by a correlation of Mach number with reservoir pressure and temperature determined from previous airflow calibrations (reference 1). These airflow calibrations consist of measured lateral surveys for a range of

tunnel operating conditions. Free-stream Mach number used in the correlation is determined from the average ratio P_0'/P_0 for each airflow calibration run (reference 3.) Dynamic pressure is then calculated from:

$$q = \frac{\gamma}{2} P_\infty M^2$$

During test OA113 (same model, but without RCS Jet Simulation; see reference 14), coefficient data scatter as high as ±20 percent was noticed at some test conditions. Since Xcp/L_b and L/D did not show this scatter, it was concluded that the coefficient scatter was caused by insufficient knowledge of dynamic pressure. Although a pitot probe was mounted in the test section, the high model angle of attack required that the probe be mounted too far from the model to provide reliable values of dynamic pressure. It was subsequently discovered that the forward model pressure (Pm_4) correlated very well with normal force. Correlations of Pm_4, normal force, and estimated dynamic pressure were then made using an iterative procedure. This same procedure was used for OA93, and the results are shown in figures 4b, 4c, and 4d.

This procedure is based upon the assumption that viscous interaction effect on normal force is on the order of 1% and can be ignored. Therefore, normal force is assumed to be linear with dynamic pressure. In addition, Pm_4 is located on the model such that it is free from flow separation and control surface deflection effects. It can also be shown that test data for Pm_4 is linear with the estimated value for dynamic pressure used for data reduction. (See figure 4d.)

DATA REDUCTION (Continued)

Test Conditions were then obtained as follows:

1. Dynamic pressure for a given run was calculated from the ratio of Pm_4/q_∞ using the measured Pm_4 for that run.

2. Pitot pressure was calculated from the theoretically established ratio of P_0'/q_∞ used in reference 3.

3. Free-stream Mach number and the other test conditions were then calculated from the ratio P_0'/P_0, using the measured values of reservoir conditions for that run and equations 5 through 8, as discussed above. For a detailed discussion of the theoretical principles and experimental substantiation for deriving the estimated dynamic pressures, see reference 14.

Other equations and methods special to this test are outlined below.

1. Calculation of viscous parameter $\bar{V}_\infty^*$ (Rockwell Method)

$$\frac{T^*}{T_\infty} = 0.5\,\frac{T(W)}{T_\infty} + (1 + 0.2\,M_\infty^2)[0.31462(\sin^2\alpha) + 0.18538]$$

$$C_\infty^* = \left[\frac{T^*}{T_\infty}\right]^{1/2}\left[\frac{T_\infty + 198.6}{T^* + 198.6}\right]$$

$$\bar{V}_\infty^* = \frac{M_\infty\sqrt{C_\infty^*}}{\sqrt{Re_\ell}}$$

DATA REDUCTION (Concluded)

2. Calculation of viscous parameter $\bar{V}'_\infty$ (Langley Method)

$$\frac{T'}{T_\infty} = (0.468 + 0.532\,\frac{T(W)}{T_\infty} + 0.039\,M_\infty^2)$$

$$C'_\infty = \left(\frac{T'}{T_\infty}\right)^{\frac{1}{2}} \left[\frac{5/9T_\infty + 122.1 \times 10^{-(9/T_\infty)}}{5/9T' + 122.1 \times 10^{-(9/T')}}\right]$$

$$\bar{V}'_\infty \quad \frac{M_\infty \sqrt{C'_\infty}}{\sqrt{Re_\ell}}$$

The following reference dimensions and constants were used to compute force and moment coefficient data and center of pressure locations. These values are shown in figure 2g.

Symbol	Full Scale	Model Scale
b_w	936.7 in.	9.367 in.
$\bar{c}$	474.8 in.	4.748 in.
ℓ_b	1290.3 in.	12.903 in.
S_W	2690.0 ft.^{2}	0.269 ft.^{2}
X_{MRC}	1076.7 in.	10.767 in.
S_{cav}		4.50 in.^{2}
$\bar{u}$		-0.519 in.
$\bar{v}$		0.0 in.
Y_{MRC}	0.0 in.	0.0 in.
$\bar{h}$		0.25 in.
Z_{MRC}	375.0 in.	3.75 in.

DISCUSSION OF RESULTS

Interaction effects induced by the RCS plume were obtained by taking the difference in force and moment coefficients between RCS on and RCS off (Pc = 0) runs. This was necessary because the relatively short run time did not allow time to obtain steady balance readings with the jet off and then turn the jet on, wait for the flow to reestablish and obtain another steady level. The Run Summary presented in table VII identifies the runs at each of the three test conditions, which may be paired to obtain RCS interaction effects. This table is annotated to assist the data user in interpreting the data.

Fifteen runs were made during the test; eleven yielded data. RCS timing problems were experienced in the Mach 19.4 runs 2 and 4; because these runs were repeated (runs 3 and 5), runs 2 and 4 should be treated circumspectly, if used at all. Run 7 is a repeat of the Mach 19.4, RCS on run 5 for the purpose of determining data repeatability.

On runs 6 and 13 amplifier gains on some components, as noted, were set too low. The resulting low amplitude signals impaired the resolution and thus the accuracy of the associated coefficients by a factor of 2, or more, greater than stated in the discussion on precision of data.

Test results are plotted in figures 6 through 9 with results from OA82 (Langley 31-inch CFHT). Interaction effects are plotted as a function of the inverse thrust coefficient, $\bar{q}S/T$, for an angle of attack of 30 degrees.

Figures 6 and 7 compare OA93 test results for the right hand up-

firing jets at M = 10 and 20 and $Re_\ell \approx 0.09 \times 10^6$ with OA82 test results for M = 10 and $Re_\ell \approx 1 \times 10^6$. These data indicate that there are negligible Mach number and Reynolds number effects on RCS/aerodynamic interaction in the hypersonic entry regime. The normal force interaction data are scattered, but this has been typical of all RCS effects tests to date.

Left hand down-firing jet test results are presented in figures 8 and 9. These figures compare OA93 test results at M = 10 and 20 for $Re_\ell \approx 0.09 \times 10^6$ and $Re_\ell \approx 0.7 \times 10^6$ with OA82 results at M = 10 and $Re_\ell \approx 1 \times 10^6$. There is more data scatter in these results than for the upfiring jet data and it is impossible to conclude whether a Mach number or Reynolds number effect exists. Again, the normal force data have the most scatter.

Even though the test data were not corrected for source flow, no effect is expected on the interaction results because they are obtained as a difference between RCS on and RCS off runs, thereby cancelling the source flow effect.

RCS-Off Aerodynamic Data

Although obtaining absolute aerodynamic coefficients was not the intent of this program, it is instructive to review the RCS-off coefficient data obtained in the conical nozzle. RCS-off pitch plane data are plotted as a function of the viscous interaction parameter, $\bar{V}_\infty'$, in figure 10. This plot compares the two Calspan tests in the 48-inch HST (OA93-conical nozzle and OA113-contoured nozzle) and the OA82 test data from

the Langley 31-inch CFHT. Test OA93 data are plotted with and without a conical flow correction. The correction was determined analytically using Newtonian impact pressure increments integrated over a flat plate model of the orbiter planform. The axial force correction is zero for this method. Agreement between axial force data from the OA82 Langley and OA113 and OA93 Calspan tests is very good.

While the corrected normal force and pitching moment data move closer to the parallel flow (contoured nozzle) data of tests OA82 and OA113, a discrepancy still exists. The corrected normal force data are 4 to 8% below the faired values and the corrected pitching moment is 0.002 to 0.016 above the faired values. No further attempts were made to obtain a more accurate correction.

REFERENCES

1. Description and Capabilities, Calspan Corporation, Hypersonic Shock Tunnel, April 1969.

2. Bogdan, L.,"Instrumentation Techniques for Short Duration Test Facilities," Calspan Report No. WTH-030, March 1967.

3. Rogers, C. E., "Revised HST Standard Data Reduction Program for the IBM 7044," Calspan Internal Memo, dated April 8, 1965.

4. Reece, J. W., "Shock Tube Theory for Real Air with Application to Wind Tunnel Testing and to Flight Simulation," Calspan Experimental Facilities Division, WTH-003, October 1958 (Revised August 1965.)

5. Wittliff, C., "Unpublished Normal Shock Calculations Using Duff's Computing Procedure." Aerodynamic Research Department, Calspan, about 1963.

6. Lewis, Clark H. and Burgess, E. G., "Charts of Normal Shock Wave Properties in Imperfect Air," AEDC-TDR-64-43. March 1964.

7. Hilsenrath, J., Beckett, C. W., et al., "Tables of Thermal Properties of Gases," National Bureau of Standards Circular 564, November 1955.

8. Reece, J. W., "Test Section Conditions Generated in the Supersonic Expansion of Real Air," Reader's Forum, Journal of Aerospace Science, Vol. 29, No. 5, May 1962, pp. 617-618.

9. Neel, C. A. and Lewis, Clark H., "Interpolations of Imperfect Air Thermodynamic Data, II at Constant Pressure," AEDC-TDR-64-184, Sept. 1964.

10. Hirschfelder, J. O., Curtiss, C. F., and Bird, R. G., Molecular Theory of Gases and Liquids, J. Wiley and Sons, 1954.

11. Hansen, F. C., "Approximations for Thermodynamic and Transport Properties of High-Temperature Air," NASA-TN-4150, March 1958 (Revised NASA TR-50, 1959).

12. Daileda, J. J., "Information Concerning the Preparation of Model 51-0 for Tests 0A93 and 0A113," Rockwell International Internal Letter SAS/WTO/74-181, addendum No. 1, dated August 1, 1974.

REFERENCES (Concluded)

13. DMS-DR-2113, NASA CR-134,111, "Effects of Reaction Control System Jet Flow Field Interactions on the Aerodynamic Characteristics of a 0.010-Scale Space Shuttle Orbiter Model in the Langley Research Center 31-In. CFHT-(OA85)." September 1974.

14. DMS-DR-2234, NASA CR-141,547 "Wind Tunnel Test OA113 of the 0.010-Scale Space Shuttle Orbiter Model 51-O in the Calspan Hypersonic Shock Tunnel (48-inch Leg)." June 1975.

15. SD74-SH-0057A, "Pretest Information for RCS Effects Test OA93 of the 0.010-Scale Space Shuttle Orbiter Configuration 140A/B Model 51-O in The Calspan Hypersonic (48-inch Leg)," April 23, 1974, Revised Sept. 1974.

TABLE I

TEST : 0A93, CAL I84-120 DATE : 11-22-74

TEST CONDITIONS

MACH NUMBER	REYNOLDS NUMBER (per foot)	DYNAMIC PRESSURE (pounds/sq. inch)	STAGNATION TEMPERATURE (degrees Fahrenheit)
10.75	0.607×10^6	1.958	3518
9.60	0.084×10^6	0.685	5363
19.77	0.086×10^6	0.158	4934

BALANCE UTILIZED: Calspan "E" Low-Load Balance

	CAPACITY.	ACCURACY	COEFFICIENT TOLERANCE *
NF	96.3 lbs.	±3% of measured load	
SF	62.4 lbs.	±4% "	
AF	41.0 lbs.	±3% "	
PM	60.9 in.-lbs.	±3% "	
RM	12.0 in.-lbs.	±3% "	
YM	43.1 in.-lbs.	±5% "	

COMMENTS * See Data Reduction Section

TABLE II.

TEST : [illegible]

DATA SET RUN NUMBER COLLATION SUMMARY

DATE : [illegible]

DATA SET ENTRY NUMBER	CONFIGURATION	SC. D. α	SC. D. β	PARAMETERS/VALUES δ_e	δ_{RS}	δ_{SB}	RCS	NO. OF RUNS	MACH NUMBERS (OR ALTERNATE INDEPENDENT VARIABLE) 0.0	9.60	10.75	19.17
STU001	ϕ_1	30	0	0	0	0	OFF	5		"	12	3
2								1				2
3	ϕ_2							1		15		
4	$\phi_{1,42}$						ON	3		14	3	5
5												4
6	$\phi_{1,44}$							2		8		7
RUI001	ϕ_{1N42}							1	102			
8								1	55			
9	ϕ_{N44}	↓	↓	↓	↓	↓	↓	1	167			

TEST RUN NUMBERS

CN	CA	CM	CY	CYN	CLN	PM1	PM2	PM3	PM4	MACH	ALPHA	IO
BAR	VLBAR	T^4	REFTL	SCRTC	PT	QT	P(TS)	H(W)	T(W)	C(CP)	MACH	ALPHA	IC
M(I)	P(I)	H	T	O)			P	Q(PSI)	RHO	M	MACH	ALPHA	ID

TYPE OF DATA α OR β SCHEDULES

COEFFICIENT SCHEDULES

IOVAR (1) IOVAR 2 NOV

TABLE III MODEL DIMENSIONAL DATA

MODEL COMPONENT : BODY - B_{26}

GENERAL DESCRIPTION : Configuration 140A/B orbiter fuselage

NOTE: B_{26} is identical to B_{24} except underside of fuselage has been refaired to accept W_{116}.

MODEL SCALE: 0.010 MODEL DWG: SS-A00147, Release 12

DRAWING NUMBER : VL70-000143B, -000200, -000205, -006089, -000145
VL70-000140A, -000140B

DIMENSIONS :	FULL SCALE	MODEL SCALE
Length (OML: Fwd Sta. X_o=235), In.	1293.3	12.933
Length (IML: Fwd Sta. X_o=238), In.	1290.3	12.903
Max Width (At X_o = 1528.3), In.	264.0	2.640
Max Depth (At X_o = 1464), In.	250.0	2.500
Fineness Ratio	0.264	0.264
Area - Ft^2		
Max. Cross-Sectional	340.88	0.034
Planform		
Wetted		
Base		

TABLE III (Cont'd)

MODEL COMPONENT : CANOPY - C_9

GENERAL DESCRIPTION : Configuration 3A. Canopy used with fuselage B_{26}.

MODEL SCALE: 0.010 MODEL DWG: SS-A00147, Release 12

DRAWING NUMBER : VL70-000143A

DIMENSIONS :	FULL SCALE	MODEL SCALE
Length (X_o =434.634-578)	143.357	1.434
Max Width (At X_o = 513.127)	152.412	1.524
Max Depth (At X_o = 485.0)	25.000	0.250
Fineness Ratio		
Area		
Max. Cross-Sectional		
Planform		
Wetted		
Base		

* Rev. 7/19/74

TABLE III (Cont'd)

MODEL COMPONENT: ELEVON - E_{26}

GENERAL DESCRIPTION: Configuration 140A/B orbiter elevons.
Data are for one side.

MODEL SCALE: 0.010 MODEL DWG: SS- A00148, Release 6

DRAWING NUMBER: VL70-000200, -006089, -006092

DIMENSIONS:	FULL-SCALE	MODEL SCALE
*Area - Ft^2	205.25	0.0205
* Span (equivalent), In.	346.68	3.467
* Inb'd equivalent chord , In.	115.3	1.153
* Outb'd equivalent chord, In.	55.1886	0.552
Ratio movable surface chord/ total surface chord		
* At Inb'd equiv. chord	0 214	0.214
* At Outb'd equiv. chord	0.400	0.400
Sweep Back Angles, degrees		
Leading Edge	0.00	0.00
Tailing Edge	-10.056	-10.056
Hingeline	0.00	0.00
* Area Moment (Product of area & $\bar{c}$) Ft^3	1518.271	0.0015
*Mean Aerodynamic Chord, In.	88.777	0.888

TABLE III (Cont'd)

MODEL COMPONENT : BODY FLAP - F_7

GENERAL DESCRIPTION : Configuration 140A/B orbiter body flap

MODEL SCALE: 0.010 MODEL DWG: SS-A00147, Release 12

DRAWING NUMBER : VL70-000140A, -000145

DIMENSIONS :	FULL SCALE	MODEL SCALE
Length(X_o =1520 to X_o =1613), In.	93.000	0.930
Max Width, In.	262.00	2.620
Max Depth (X_o = 1520), In.	23.00	0.230
Fineness Ratio		
Area - Ft^2		
Max. Cross-Sectional		
Planform	142.6	0.014
Wetted		
Base	41.847	0.0042

Model dim. measured from model sta. 15.20

TABLE III (Cont'd)

MODEL COMPONENT: OMD POD - M_{15}

GENERAL DESCRIPTION: Configuration 3A - Modified RCS simulation with nonmetric RCS engine housing and nozzles. Same geometry as M_7 forward of Station X_o = 1502.

MODEL SCALE: 0.010

DRAWING NUMBER: VL70-000140A, -000145

DIMENSIONS:	FULL SCALE	MODEL SCALE
Length (OMS Fwd Sta X_o = 1233.), In.	269.0	2.690
Max Width (At X_o = 1450.0), In.	94.5	0.945
Max Depth (At X_o = 1493.0), In.	110.0	1.100
Fineness Ratio		
Area		
Max. Cross-Sectional		
Planform		
Wetted		
Base		

TABLE III (Cont'd)

MODEL COMPONENT: NOZZLES - N_{43}

GENERAL DESCRIPTION: RCS nozzle providing left-hand pitch-down control to simulate reentry.

MODEL SCALE: 0.010

DRAWING NO.: SS-A01160-15

DIMENSIONS:	MODEL SCALE
Flight dynamic pressure simulation - PSF	5
Cant angle - Deg.	
Aft	12
Outboard	20
Diameter - In.	
Exit	0.129
Throat	0.0465
Area - In^2	
Exit	0.013
Throat	0.002
Area ratio	7.697
No. of nozzles	2

TABLE III (Cont'd)

MODEL COMPONENT: NOZZLE - N_{44}

GENERAL DESCRIPTION: RCS nozzle providing right-hand pitch-up control to simulate reentry.

MODEL SCALE: 0.010

DRAWING NO.: SS-A01160-9

DIMENSIONS:	MODEL SCALE
Flight dynamic pressure simulation - PSF	5
Cant angle - deg.	
Aft	0
Outboard	0
Diameter, In.	
Exit	0.129
Throat	0.0465
Area - $In.^2$	
Exit	0.013
Throat	0.002
Area ratio	7.697
No. of nozzles	2

TABLE III (Cont'd)

MODEL COMPONENT: MPS NOZZLES - N_{76}

GENERAL DESCRIPTION: Configuration 3A and 4 MPS nozzles

Two lower nozzles only. Same as N_{39}, except MPS engine heatshields added.

MODEL SCALE: 0.010

DRAWING NUMBER: VL70-005106A

DIMENSIONS:	FULL SCALE	MODEL SCALE
MACH NO.		
Length - In.		
Gimbal Point to Exit Plane	157.00	1.570
Throat to Exit Plane	99.2	0.992
Diameter - In.		
Exit	94.00	0.940
Throat	43.0	0.430
Inlet		
Area - ft^2		
Exit	48.193	0.0048
Throat		
Gimbal Point (station) In.		
Upper Nozzle		
X		
Y		
Z		
Lower Nozzles		
X	1468.2	14.682
Y	±53.0	±0.530
Z	342.7	3.427
Null Position - Deg.		
Upper Nozzle		
Pitch		
Yaw		
Lower Nozzle		
Pitch	10	10
Yaw	3°30'	3°30'

TABLE III (Cont'd)

MODEL COMPONENT: RUDDER - R_5

GENERAL DESCRIPTION: Configuration 140C orbiter rudder (identical to configuration 140A/B rudder).

MODEL SCALE: 0.010

DRAWING NUMBER: VL70-000146B, -000095

DIMENSIONS:	FULL-SCALE	MODEL SCALE
Area - Ft^2	100.15	0.00100
Span (equivalent), In.	201.00	2.010
Inb'd equivalent chord , In.	91.585	0.916
Outb'd equivalent chord , In.	50.833	0.508
Ratio movable surface chord/ total surface chord		
At Inb'd equiv. chord	0.400	0.400
At Outb'd equiv. chord	0.400	0.400
Sweep Back Angles, degrees		
Leading Edge		
Tailing Edge	26.25	26.25
Hingeline	34.83	34.83
Area Moment (Normal to hingeline) (Product of area & $\bar{c}$) Ft^3	610.92	0.0006
Mean Aerodynamic Chord, In.	73.2	0.732

TABLE III (Cont'd)

MODEL COMPONENT: VERTICAL - V_8

GENERAL DESCRIPTION: Configuration 140C orbiter vertical tail (identical to configuration 140A/B vertical tail).

MODEL SCALE: 0.010

DRAWING NUMBER: VL70-000140C, -000146B

DIMENSIONS:	FULL SCALE	MODEL SCALE
TOTAL DATA		
Area (Theo) - Ft^2		
Planform	413.253	0.0413
Span (Theo) - In.	315.72	3.157
Aspect Ratio	1.675	1.675
Rate of Taper	0.507	0.507
Taper Ratio	0.404	0.404
Sweep-Back Angles, Degrees.		
Leading Edge	45.00	45.000
Trailing Edge	26.25	26.25
0.25 Element Line	41.13	41.13
Chords:		
Root (Theo) WP	268.50	2.685
Tip (Theo) WP	108.47	1.085
MAC	199.81	1.998
Fus. Sta. of .25 MAC	1463.35	14.634
W.P. of .25 MAC	635.52	6.355
B.L. of .25 MAC	0.00	0.00
Airfoil Section		
Leading Wedge Angle - Deg.	10.00	10.00
Trailing Wedge Angle - Deg.	14.92	14.92
Leading Edge Radius	2.00	0.020
Void Area	13.17	0.0013
Blanketed Area	0.0	0.0

TABLE III (Concluded)

MODEL COMPONENT: $WING\text{-}W_{116}$

GENERAL DESCRIPTION: Configuration 4

NOTE: Identical to W_{114} except airfoil thickness. Dihedral angle is along trailing edge of wing. Geometric twist = 0.

MODEL SCALE: 0.010

TEST NO. DWG. NO. VL70-000140A, -000200

DIMENSIONS:	FULL-SCALE	MODEL SCALE
TOTAL DATA		
Area (Theo.) Ft^2 Planform	2690.00	0.2690
Span (Theo In.	936.68	9.367
Aspect Ratio	2.265	2.265
Rate of Taper	1.177	1.177
Taper Ratio	0.200	0.200
Dihedral Angle, degrees	3.500	3.500
Incidence Angle, degrees	0.500	0.500
Aerodynamic Twist, degrees		
Sweep Back Angles, degrees		
Leading Edge	45.000	45.000
Trailing Edge	-10.056	-10.056
0.25 Element Line	35.209	35.209
Chords:		
Root (Theo) B.P.0.0.	689.24	6.892
Tip, (Theo) B.P.	137.85	1.379
MAC	474.81	4.748
Fus. Sta. of .25 MAC	1136.83	11.368
W.P. of .25 MAC	290.58	2.906
B.L. of .25 MAC	182.13	1.821
EXPOSED DATA		
Area (Theo) Ft^2	1751.50	0.175
Span, (Theo) In. BP108	720.68	7.207
Aspect Ratio	2.059	2.059
Taper Ratio	0.245	0.245
Chords		
Root BP108	562.09	5.621
Tip 1.00 $\frac{b}{2}$	137.85	1.379
MAC	392.83	3.928
Fus. Sta. of .25 MAC	1185.98	11.860
W.P. of .25 MAC	294.30	2.943
B.L. of .25 MAC	251.77	2.518
Airfoil Section (Rockwell Mod NASA) XXXX-64		
Root $\frac{b}{2}$ =	0.113	0.113
Tip $\frac{b}{2}$ =	0.120	0.120
Data for (1) of (2) Sides		
Leading Edge Cuff Planform Area Ft^2	113.18	0.011
Leading Edge Intersects Fus M. L. @ Sta	500.0	5.000
Leading Edge Intersects Wing @ Sta	1024.0	10.240

TABLE IV
NOZZLE GEOMETRY

NOZZLE BLOCK NO.	PART NO.	THROAT		EXIT		AREA RATIO	NOTES
		DIAMETER (IN.)	AREA (IN^2)	DIAMETER (IN.)	AREA (IN^2)		
N_{43}	-15	0.0465	0.001698	0.129	0.013069	7.697	L/H Pitch down. Sim. re-entry q_∞ = 5 PSF canted 12^o AFT & 20^o outboard R/H pitch up Sim. re-entry q_∞ = 5 PSF.
N_{44}	-9						(see table III)

NOTE: NOZZLE CONFIGURATIONS ARE SHOWN IN FIGURE 2C AND NOZZLE CALIBRATION RESULTS ARE SHOWN IN FIGURE 2R. EACH NOZZLE BLOCK HAS TWO NOZZLES.

TABLE V RCS NOZZLE SIMULATION

q_∞ = 5 PSF ENTRY TRAJECTORY POINT SIMULATION

A. Free Stream Conditions		Free Flight	Test Condition 1	2	3
Dynamic Pressure	q_∞, psf	5	206	58.8	19.8
Mach Number,	M_∞	29.5	10.7	10.4	19.8
*Reynolds Number	$Re_\infty \times 10^6$	0.16	0.967	0.0925	0.0326
Altitude	h, ft	280,000	-	-	-
B. RCS Jet Characteristics		**Prototype**			
Chamber Pressure	Pc, psia	150	1600	700	176
Chamber Temp.	Tc ^{o}R	5450	530	530	530
Average Specific Heat	γ	1.232	1.4	1.4	1.4
Expansion Ratio		20	8.169	8.169	8.169
Nozzle Lip angle	θ_j, deg.	9	34.5	34.5	34.5
Exit Area	Ae, in^2	72.382	0.013	0.013	0.013
Exit Mach No.	Mj	3.93	3.7	3.7	3.7
Exit Pressure	Pj, psi	0.643	16	6.93	1.74
Mass Flow rate	mj, lbm/sec	3.287	0.0594	0.026	0.00631
Momentum	m_j, U_j, lbs	903.46	3.7	1.597	0.41
Thrust	TH, lbs.	950	3.914	1.687	0.4332
C. Jet to Free Stream Parameters (S ref = 1 ft.^{2})		**Full Scale Free Flight**			
Thrust Ratio	TH/q_∞ Sref	190	190	190	190
Mass Flow Ratio	mj/[illegible]	[illegible]	238	394	354
Momentum ratio	mj Uj/q_∞ Sref	180	180	180	180
Pressure ratio	Pj/P_∞	11400	855	950	4000
Plume Shape		boundary up to impact station	(matched)	(matched)	(matched)

* Reynolds number based on orbiter length
o_{r_b} = 107.5 ft.

Table VI Summary of Test Conditions

$\delta_e = 0°$ $\delta_{BF} = 0°$

RCS ON/OFF	RUN NO.	α (DEG)	MACH	VBAR	PM_4 (PSIA)	Q #/IN^2	C_N	N LBS
OFF	2	30	19.51	0.05111	0.09744	0.1700	0.7030	4.61156
OFF	3	30	19.51	0.05243	0.09089	0.1579	0.7723	4.7237
OFF	6	30	9.64	0.02495	0.4815	0.6663	0.7493	19.4142
OFF	15	29.97	9.62	0.02475	0.4664	0.6726	0.7501	19.5430
OFF	12	30	10.46	0.01034	1.507	2.159	0.7427	62.1127
ON	4	30	19.58	0.05136	0.1731	0.1680	0.7490	4.8742
ON	5	30	19.32	0.05111	0.1147	0.1664	0.6576	4.2387
ON	7	30	19.16	0.04855	0.1232	0.1856	0.7039	5.0606
ON	8	29.98	9.59	0.02438	0.5022	0.6963	0.7240	19.5277
ON	14	29.98	9.56	0.02435	0.5132	0.6937	0.7529	20.2313
ON	13	29.98	10.53	0.01036	1.674	2.260	0.7699	65.6102

TABLE VII
RUN SUMMARY
$\alpha = 30^{o}$

Run No.	M_∞	Nominal Re/ft $X10^{-6}$	P_c (Psia)	Remarks
2	19.4	0.09	0	Data traces not steady; suspect Valcor valve inadvertently actuated
3	19.4	0.09	0	
4.	19.4	0.09	175	RCS plenum pressure did not stabilize during run
5	19.4	0.09	175	
6	9.6	0.084	0	Low amplitude data traces on Y, n, l, A; amplifier gains too low
7	19.4	0.09	175	
8	9.6	0.084	410	
12	10.5	0.65	0	
13	10.5	0.65	1530	Low amplitude data trace on yawing moment; amplifier gain too low
14	9.6	0.084	690	
15	9.6	0.084	0	RCS hardware removed to determine flow interference effects

Runs 1, 10, 11: No data; data acquisition system trigger problems.
Run 9: Mylar diaphragm apparently struck model.

Notes:

1. Positive directions of force coefficients, moment coefficients, and angles are indicated by arrows.
2. For clarity, origins of wind and stability axes have been displaced from the center of gravity.

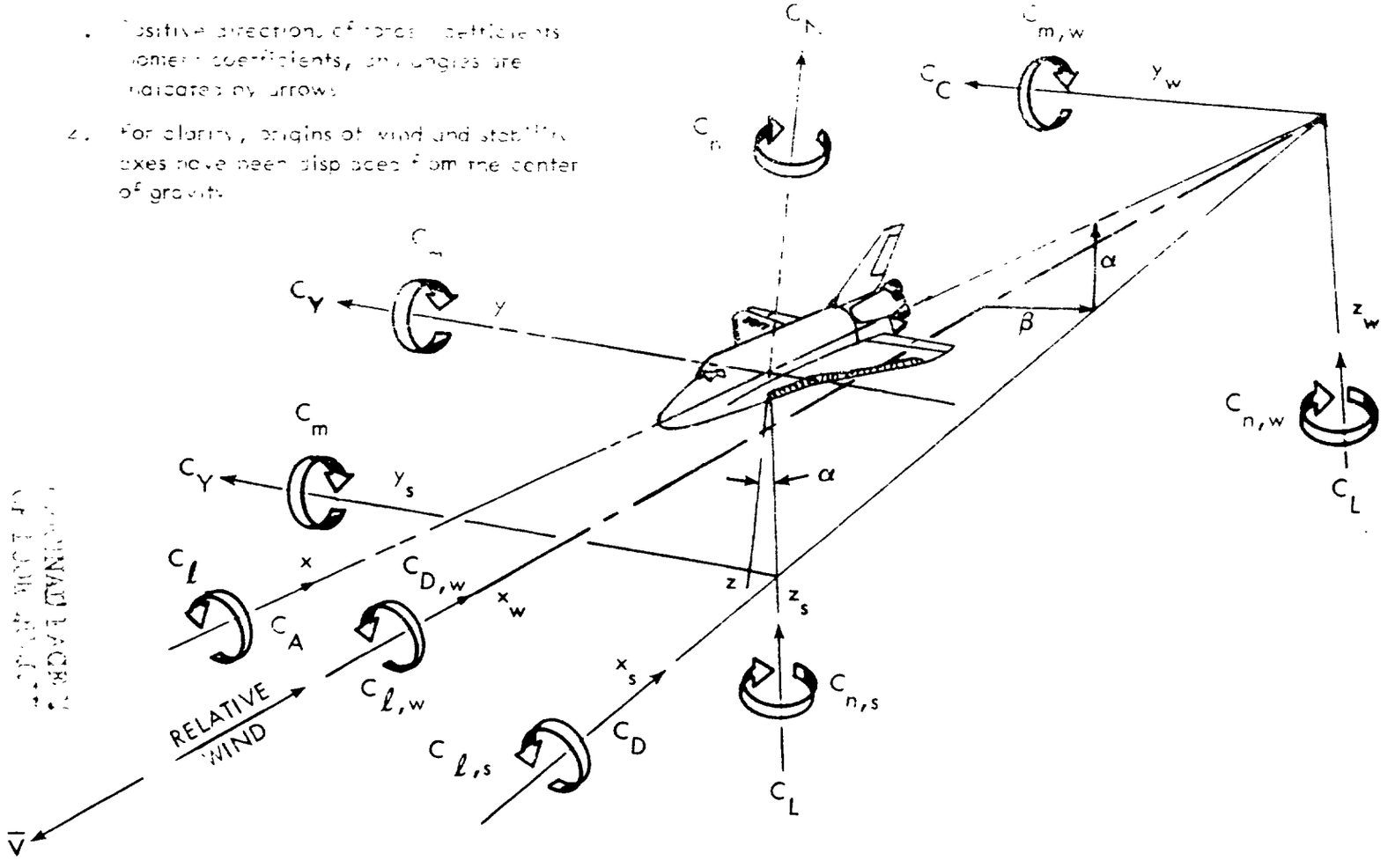

Figure 1. Axis Systems

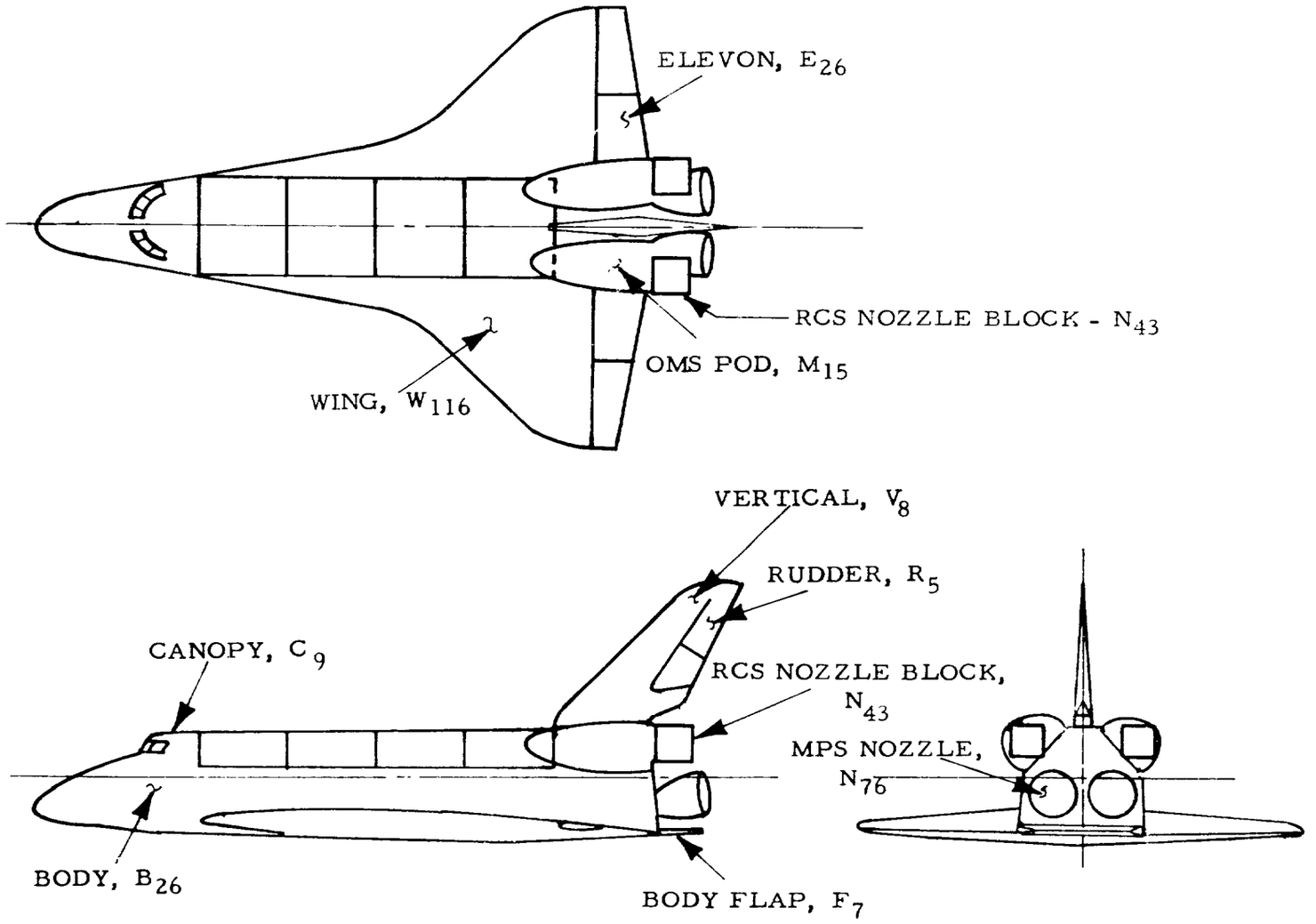

a. Orbiter Three View

Figure 2. Model Sketches

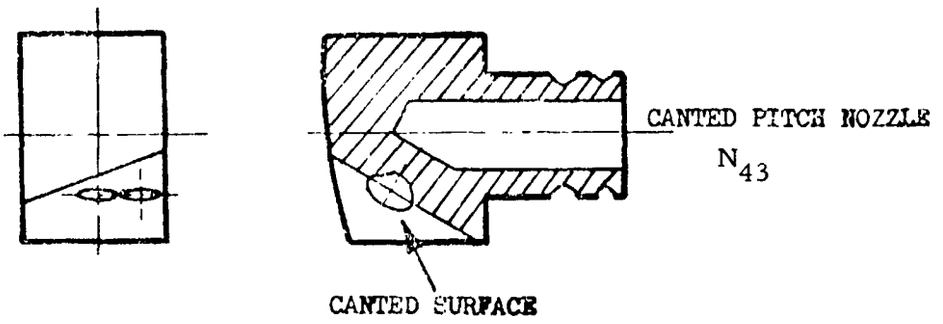

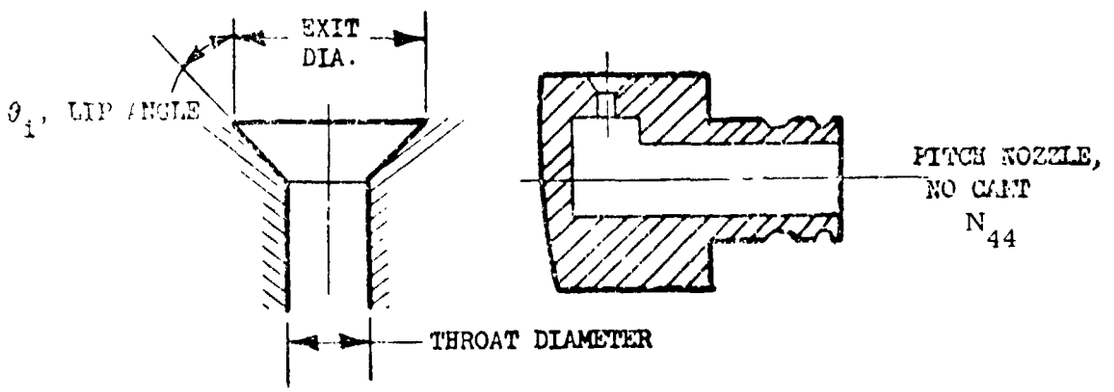

b. RCS Nozzle Configurations
Figure 2. Model Sketches (Cont'd)

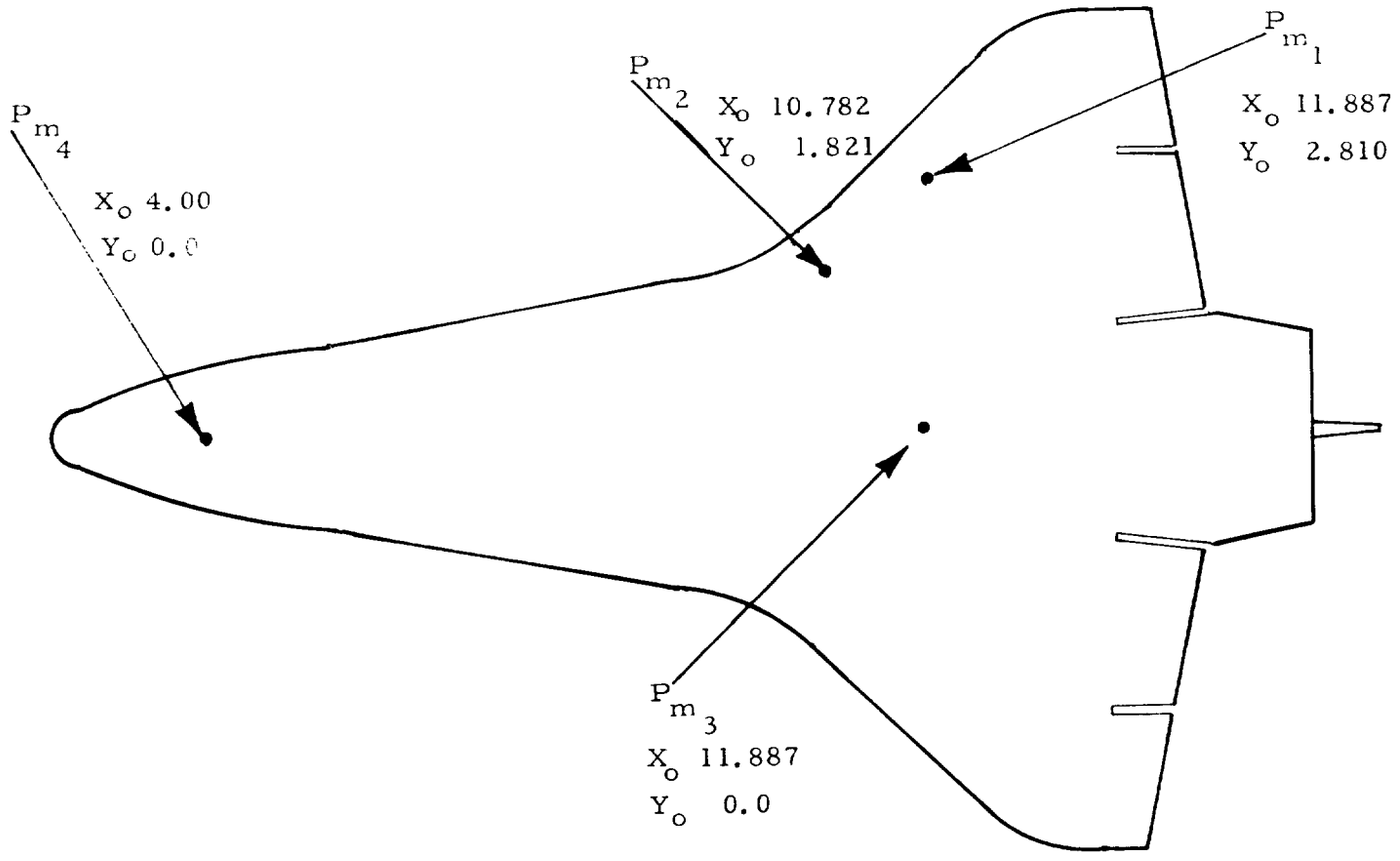

NOTE: ALL ORBITER COORDINATES ARE MODEL SCALE, INCHES

c. Static Pressure Tap Locations

Figure 2. Continued

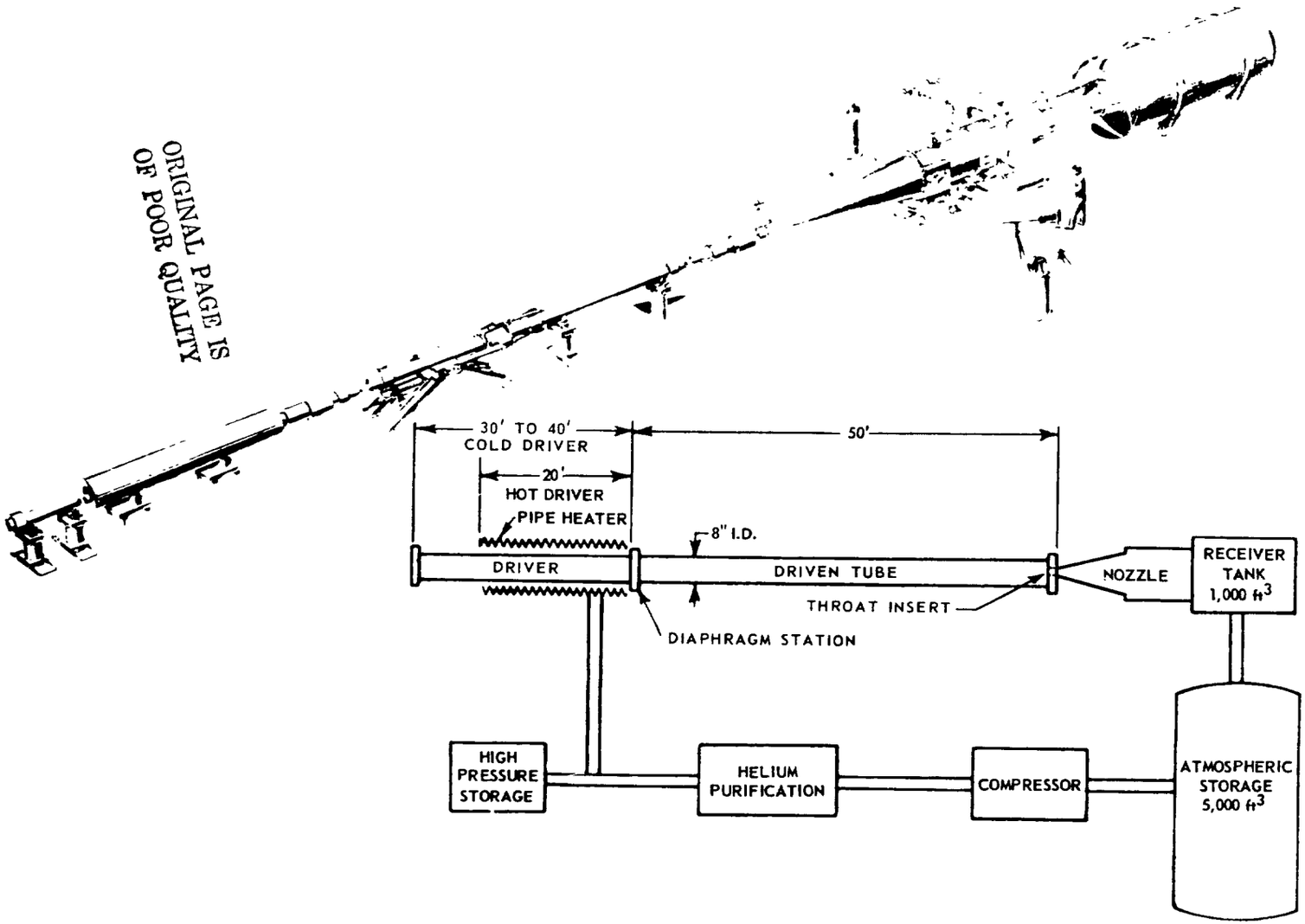

d. Basic Components of the Calspan Hypersonic Shock Tunnel - 48" Leg
Figure 2. Model Sketches (Cont'd)

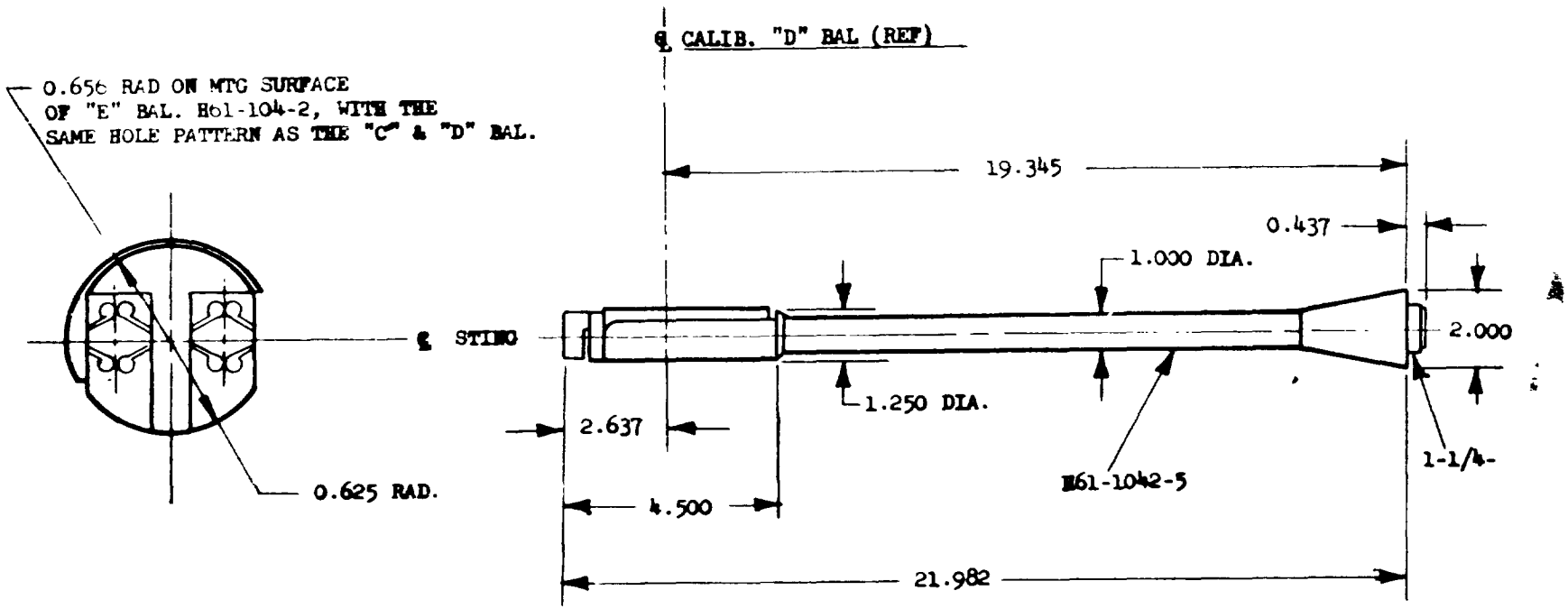

e. Calspan "E" Balance Assembly, 6 component-crystal

Figure 2. Model Sketches (Cont'd)

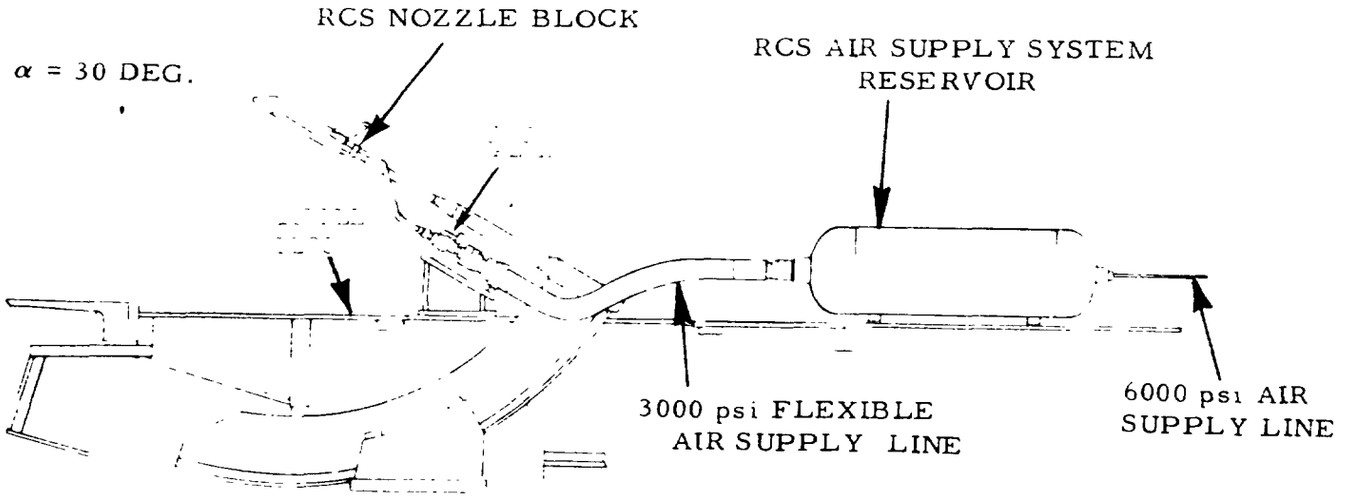

f. Installation of Model 51-O in the Calspan Hypersonic Shock Tunnel (48 Inch Leg)

Figure 2. Model Sketches (Cont'd)

REFERENCE	DIMENSIONS (FS)
AREA	S_w = 2690 FT^2
MAC	C = 474.8 IN.
C.G.	X_o = 1076.7 IN.
	Z_o = 375 IN.
SPAN	b_w = 936.68 IN.
LENGTH	ℓ_B = 1290.3 IN.

ALL DIMENSIONS IN INCHES
FULL SCALE

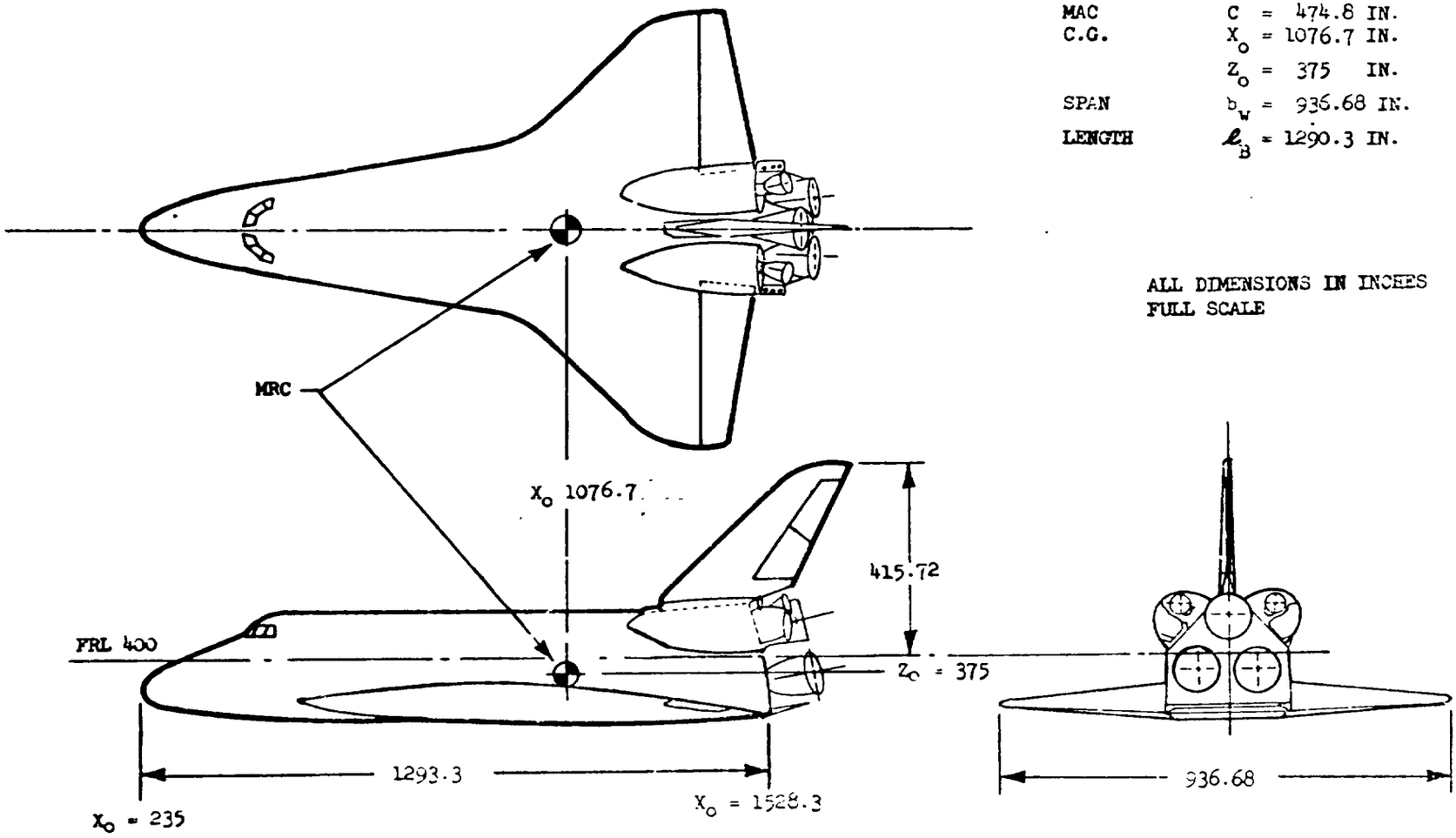

s. OV Orbiter Configuration 140A/B
Figure 2. Model Sketches (Concluded)

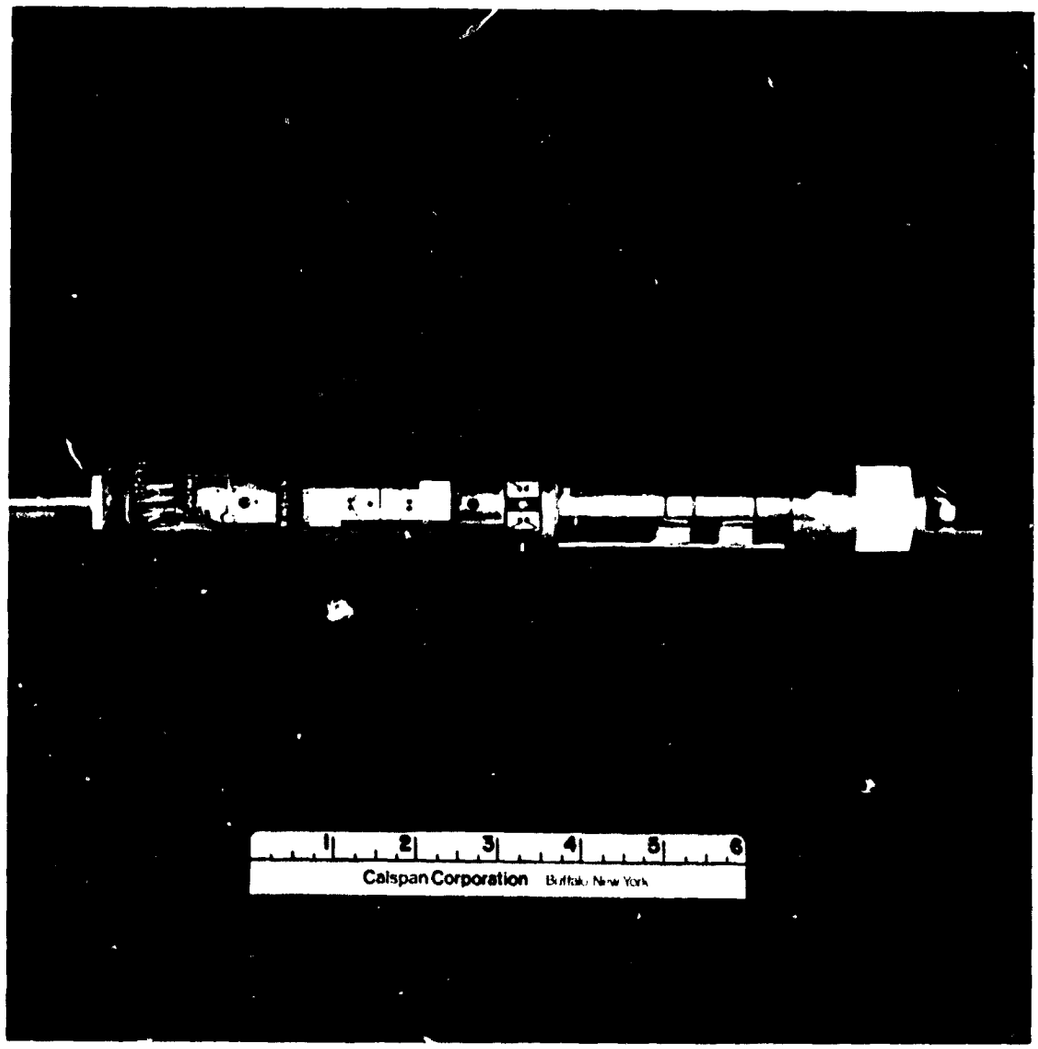

a. Right side view of Calspan "E" force balance assembly with acceleration bracket.

Figure 2. Model Photographs

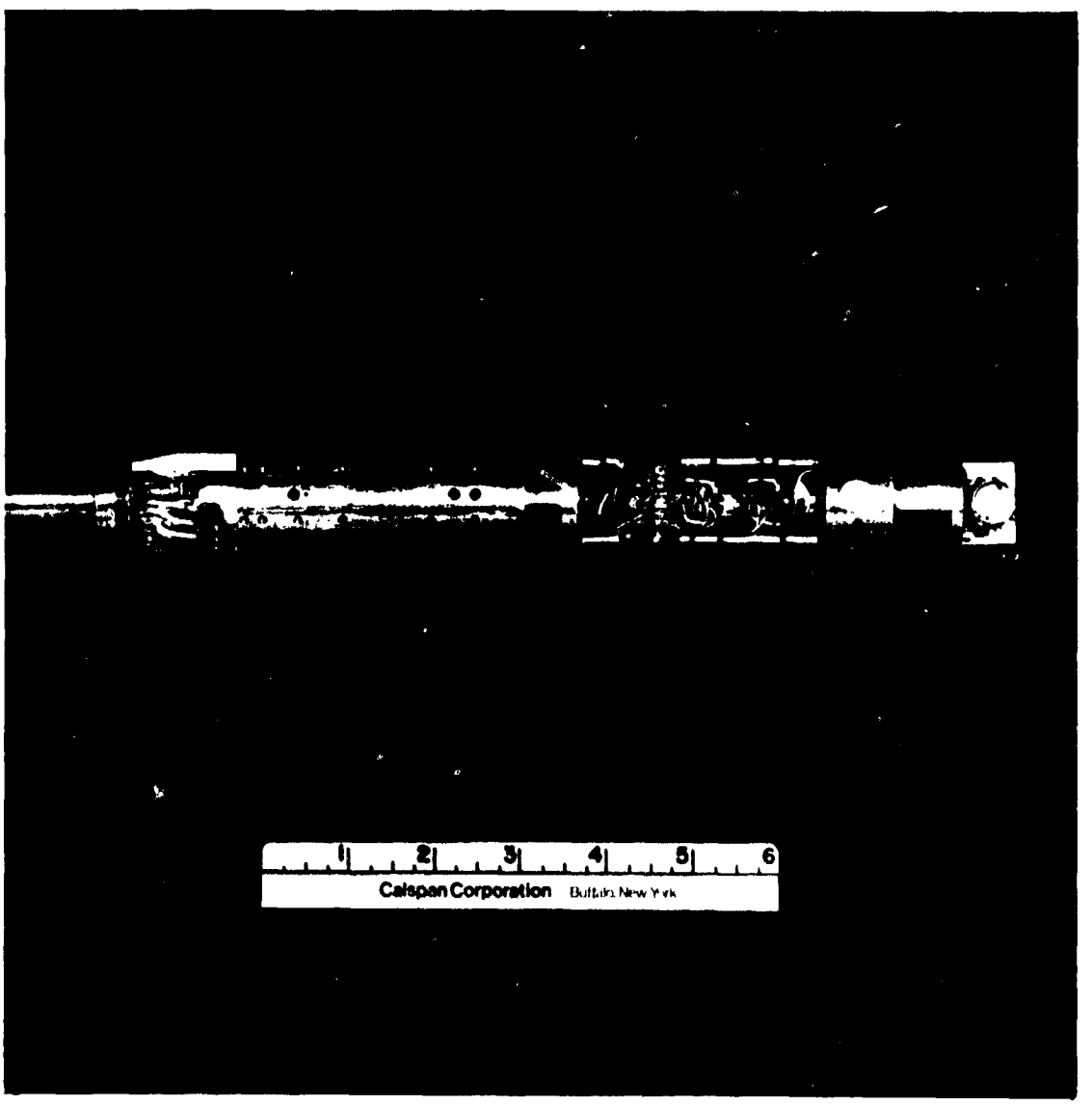

b. Top view of Calspan "E" force balance assembly and acceleration bracket.

Figure 3. Model Photographs - (Cont'd)

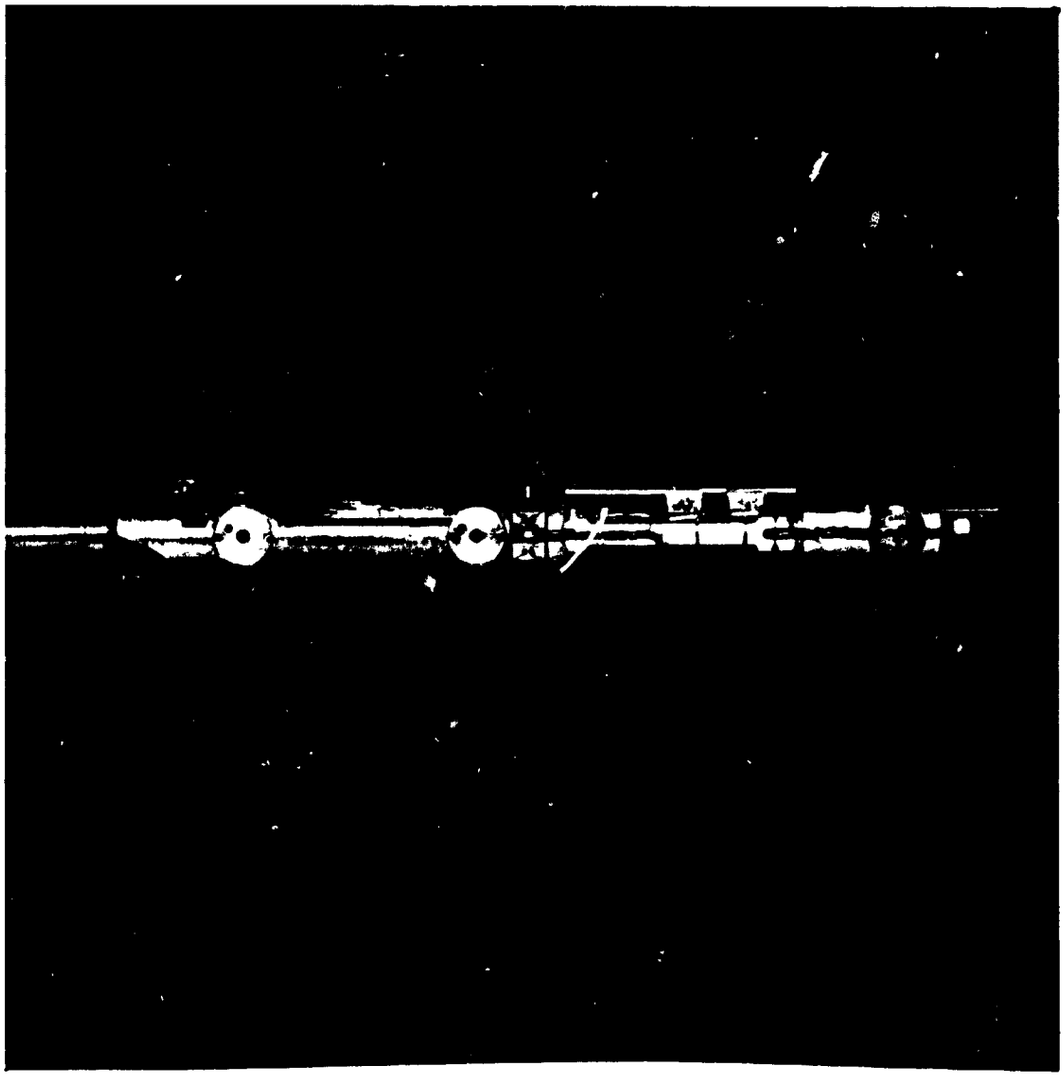

c. Left side view of Calspan "E" force balance assembly and acceleration bracket.
Figure 3. Model Photographs - (Cont'd)

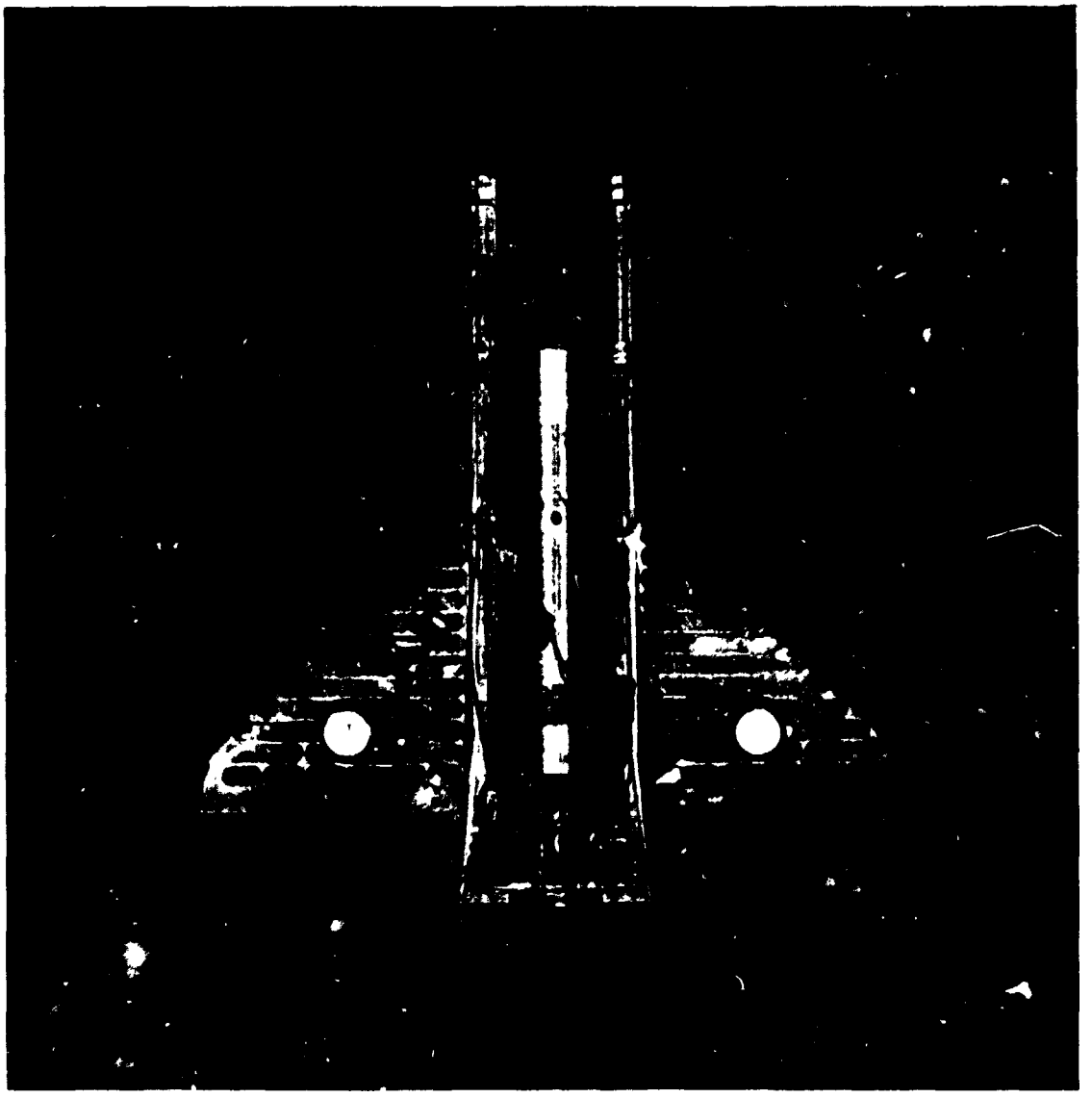

d. Top view of model showing wing accelerometer, on-board amplifiers, and Field Effects Transisters (FETS).
Figure 3. Model Photographs - (Cont'd)

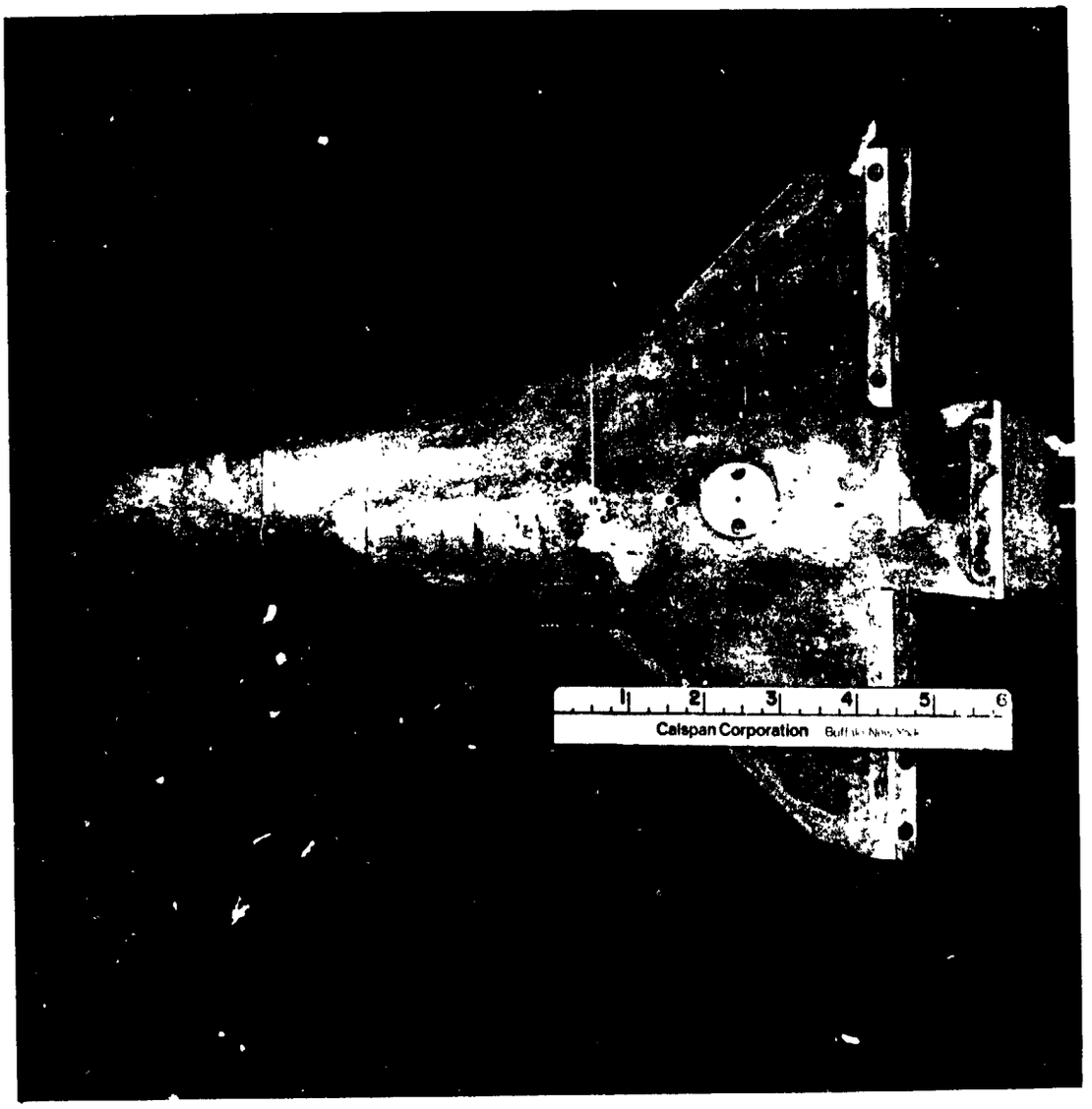

f. Bottom view of model showing static pressure orifices, [illegible] load pan holes, and transducer mount for PM.

Figure 3. Model Photographs - (Cont'd)

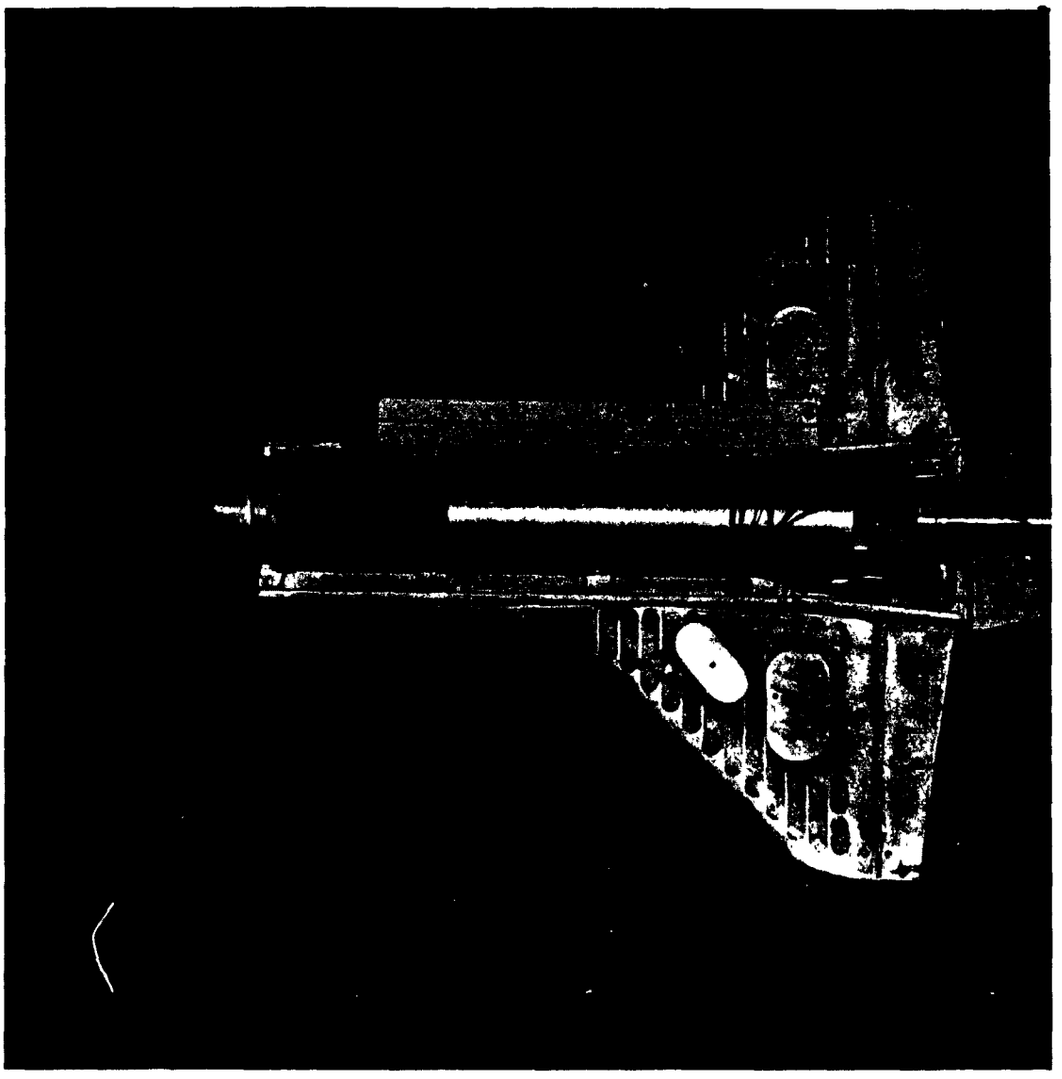

g. Top view showing model mounted on sting-balance assembly and cavity pressure transducer on forward right side of balance housing.

Figure 3. Model Photographs - (Cont'd)

h. Side view of Model 51-O mounted on Calspan sting, without nonmetric RCS hardware installed.
Figure 3. Model Photographs - (Cont'd)

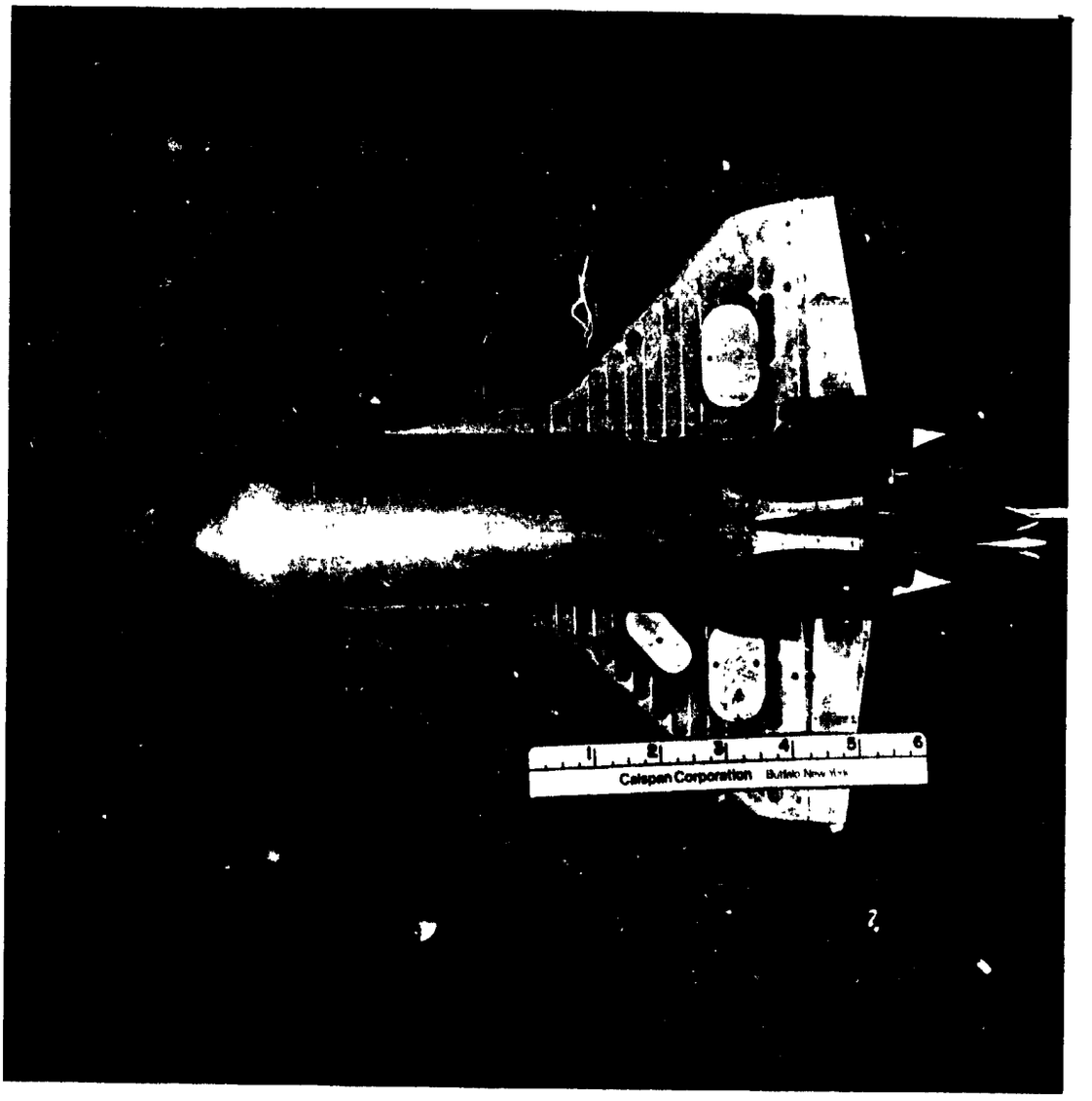

i. Top view of Model 51-0 mounted on Calspan sting, without non-metric RCS hardware installed.
Figure 3. Model Photographs - (Cont'd)

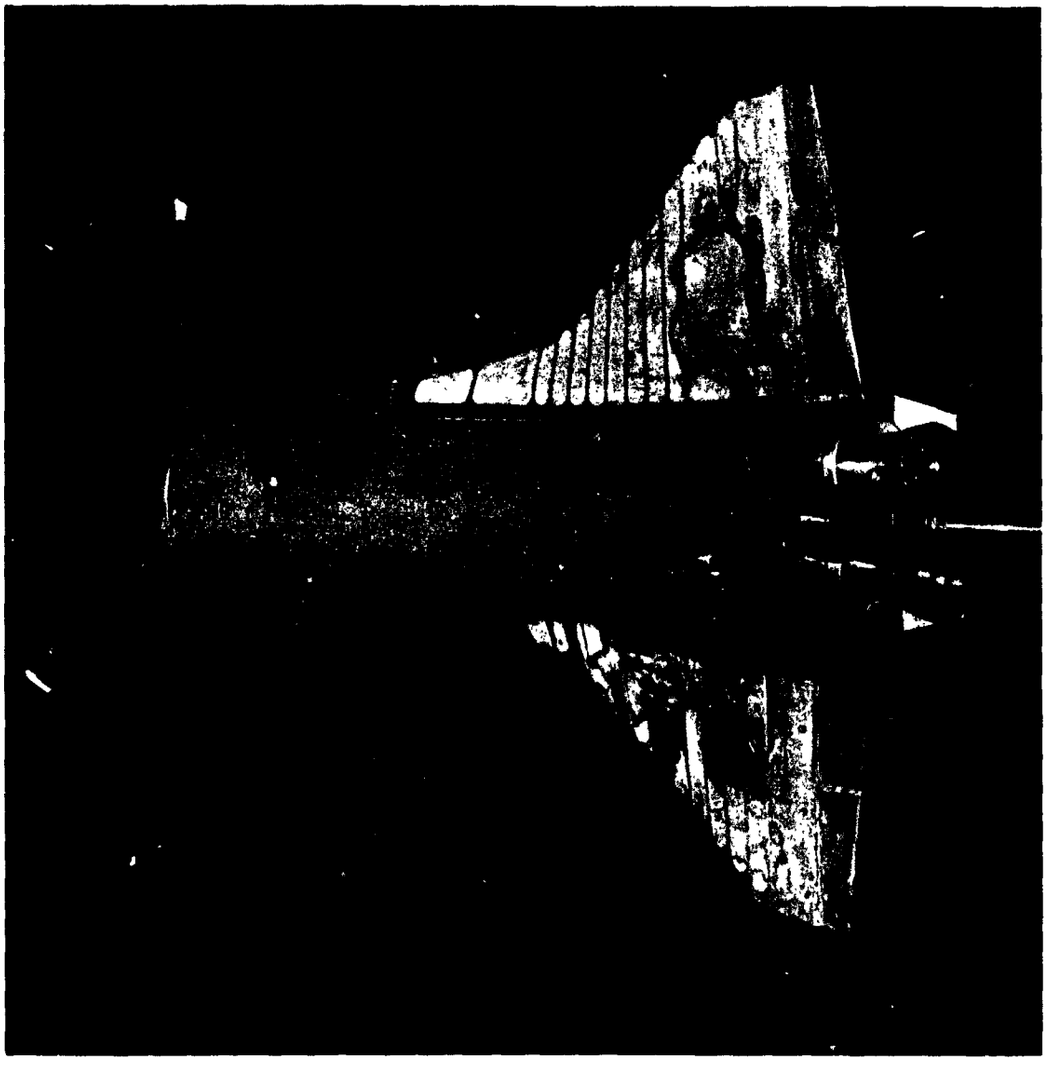

j. Close-up of aft end of Model 51-O showing clearance between sting and MPS nozzles. NOTE: non-metric RCS hardware not installed.
Figure 3. Model Photographs - (Cont'd)

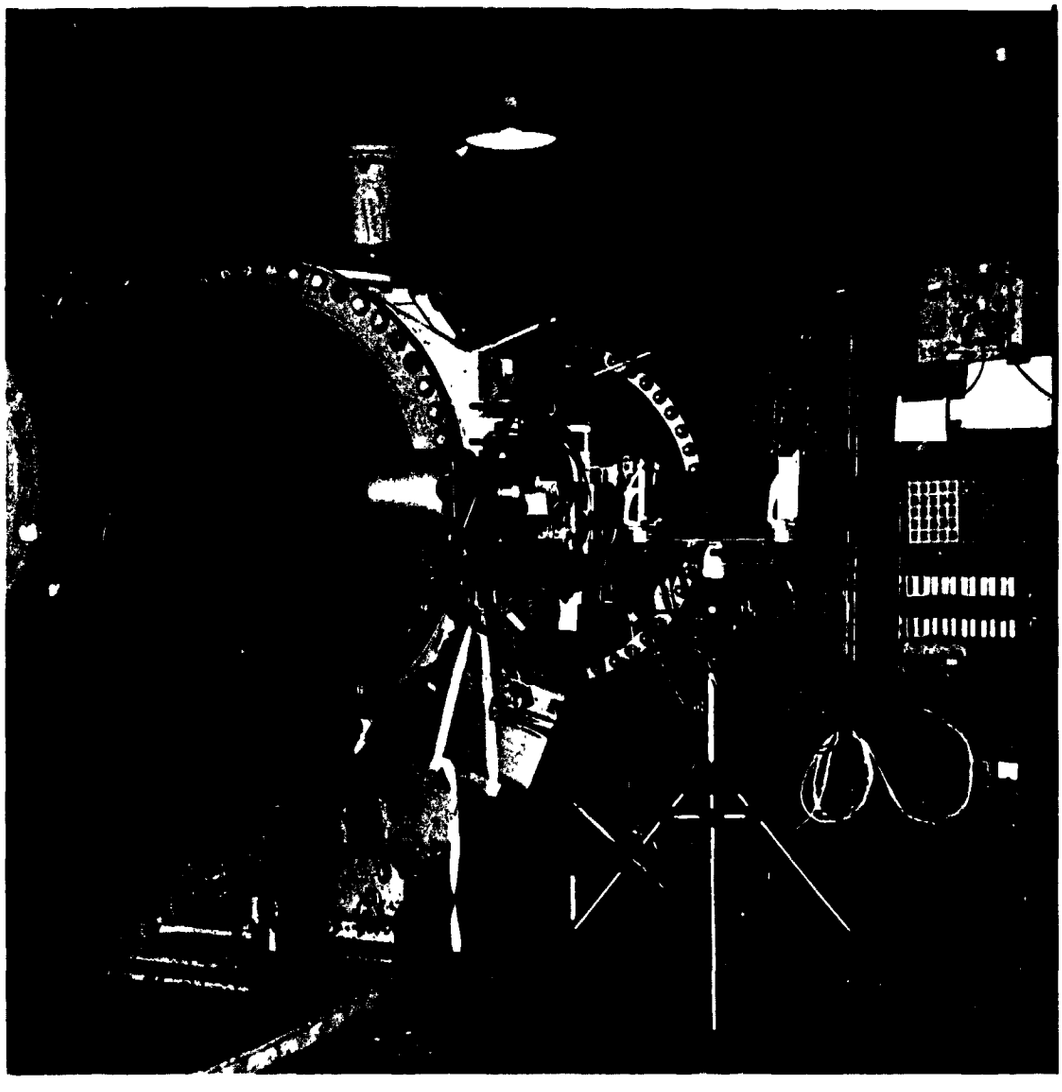

k. External view of Calspan 48" Hypersonic Shock Tunnel (HST) showing from left to right, "D" nozzle and test section, Schlieren equipment, and analog computer.
Figure 3. Model Photographs - (Cont'd)

1. Left side view of pitot rake and Model 51-0 (α = 30°) and PCS hardware, installed in Calspan 48" HST.

Figure 3. Model Photographs - (Cont'd)

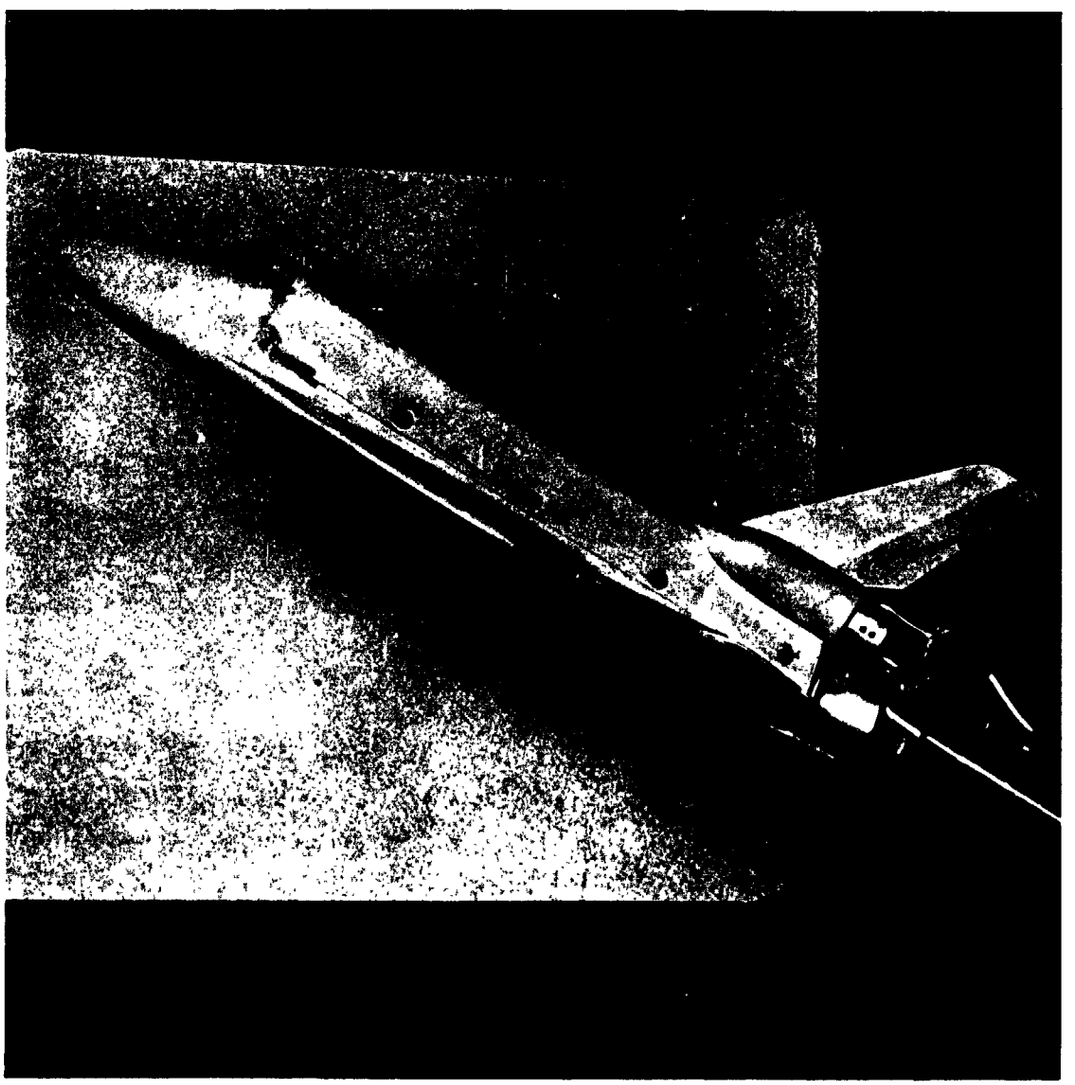

m. Close-up view of left side of Model 51-O and RCS hardware, installed in Calspan 48" HST.
Figure 3. Model Photographs - (Cont'd)

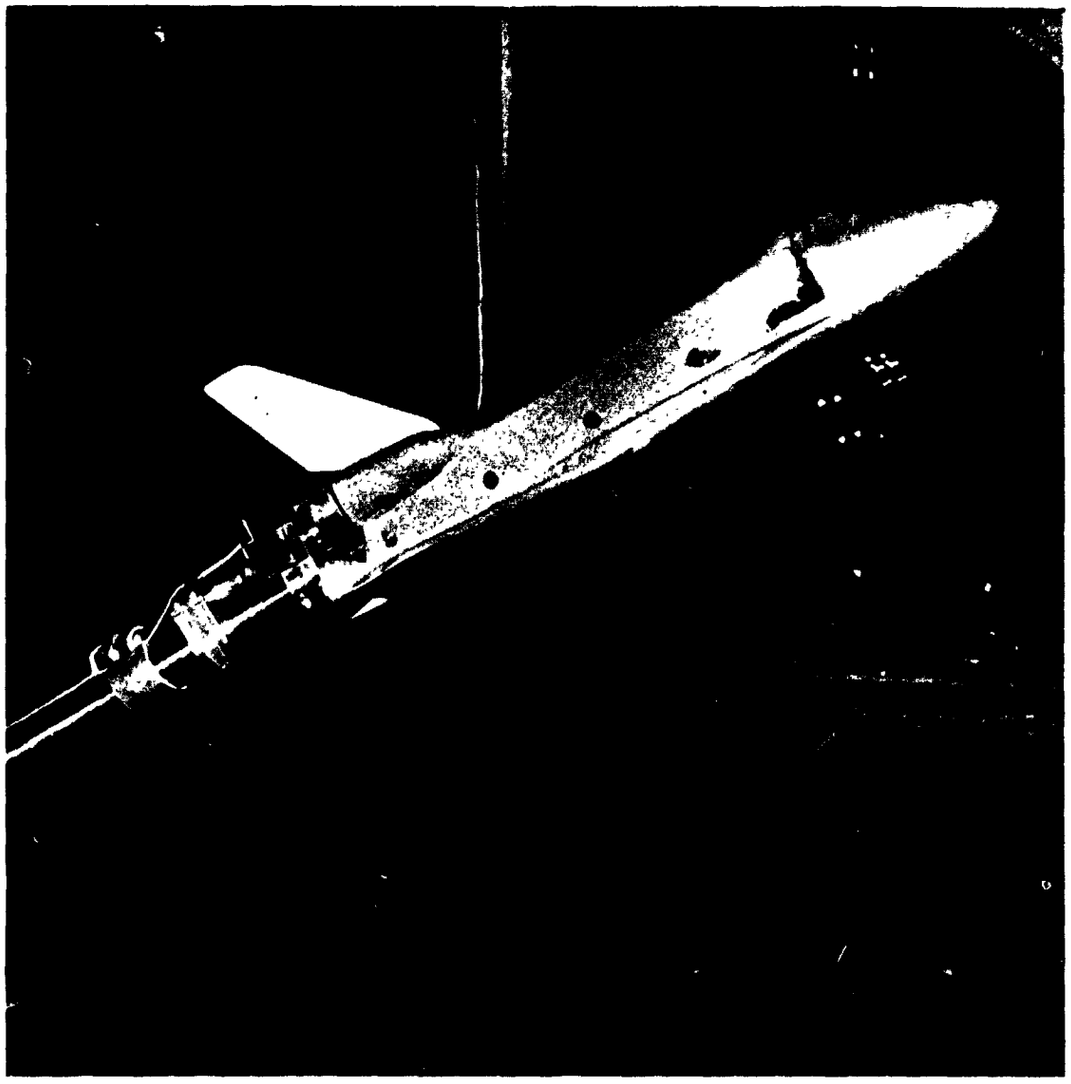

n. Right side view of Model 51-O and RCS hardware, installed in Calspan 48" HST.

Figure 3. Model Photographs - (Cont'd)

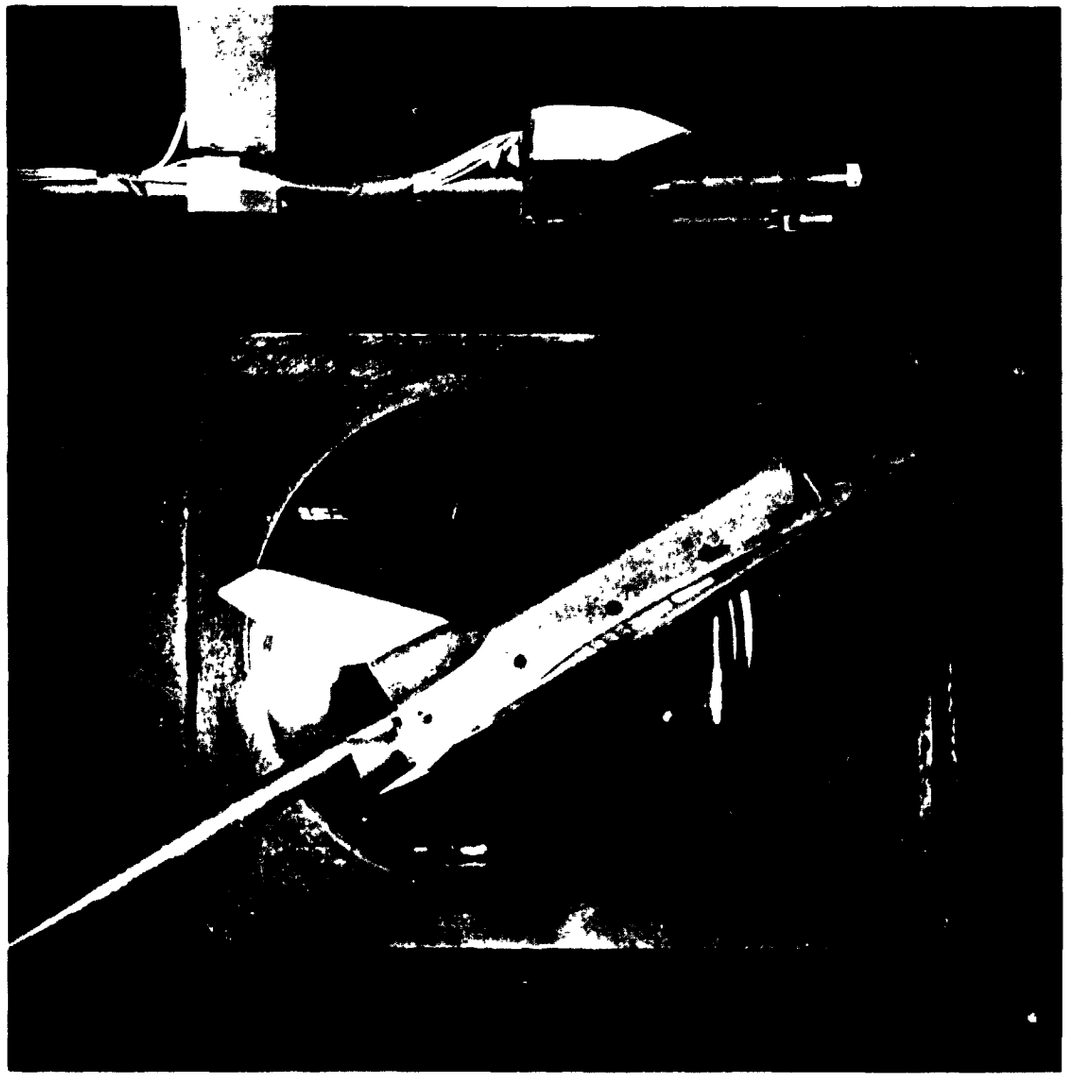

o. Right side view of pitot rake and Model 51-O (with RCS hardware removed) installed in Calspan 48" RST.

Figure 3. Model Photographs - (Cont'd)

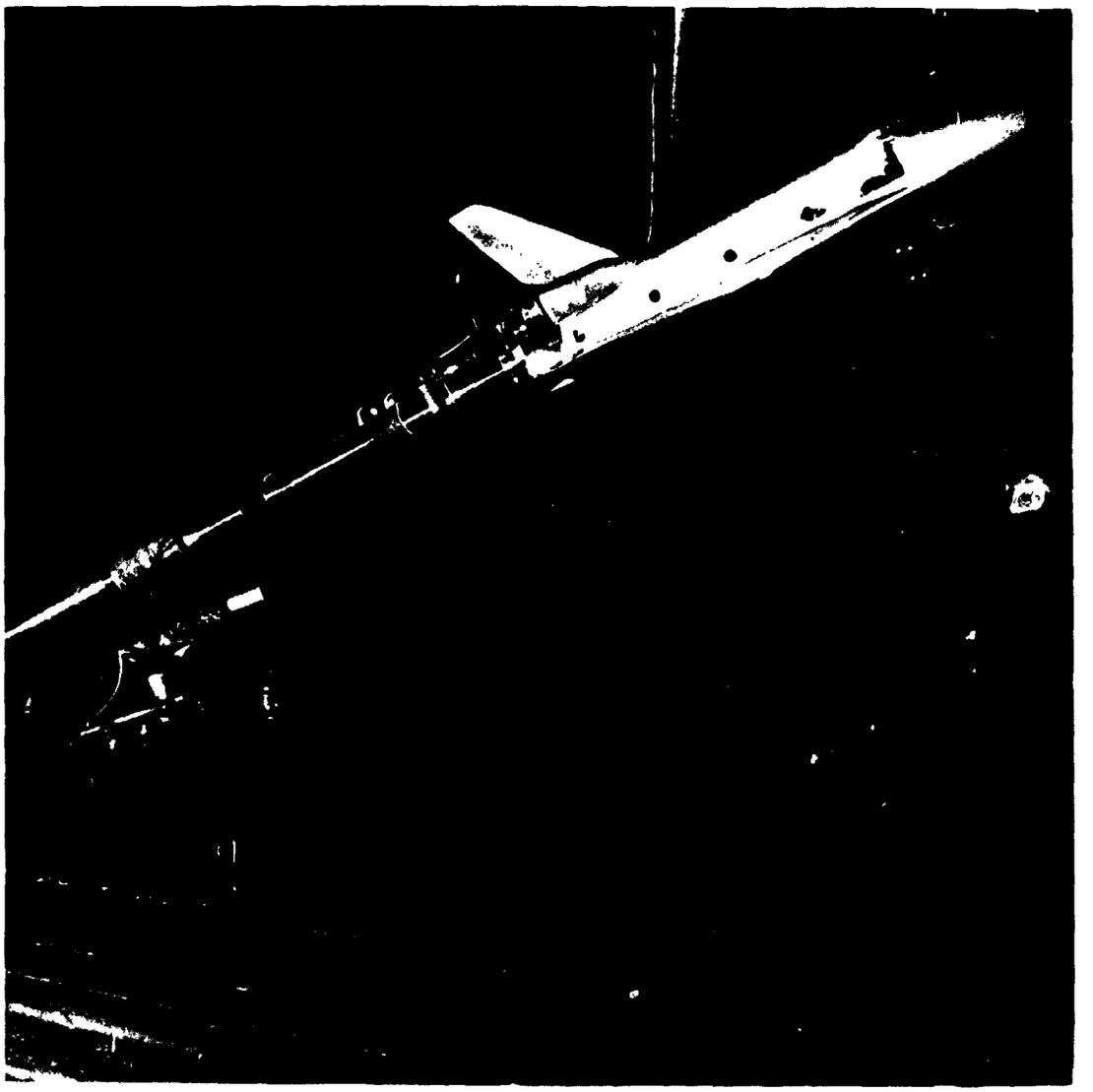

p. Right side view of Model 51-O with RCS hardware installed in Calspan 48" HST. NOTE: Mounting bracket for Valcor valve to the left of the sting.
Figure 3. Model Photographs - (Cont'd)

View of Model 51-O with RCS hardware in Calspan 48" HST. NOTE: RCS plenum tank and supply hose. Valcor valve, shown mounted on sting, was later moved to separate bracket.

Figure 5. Model Photographs - (Cont'd)

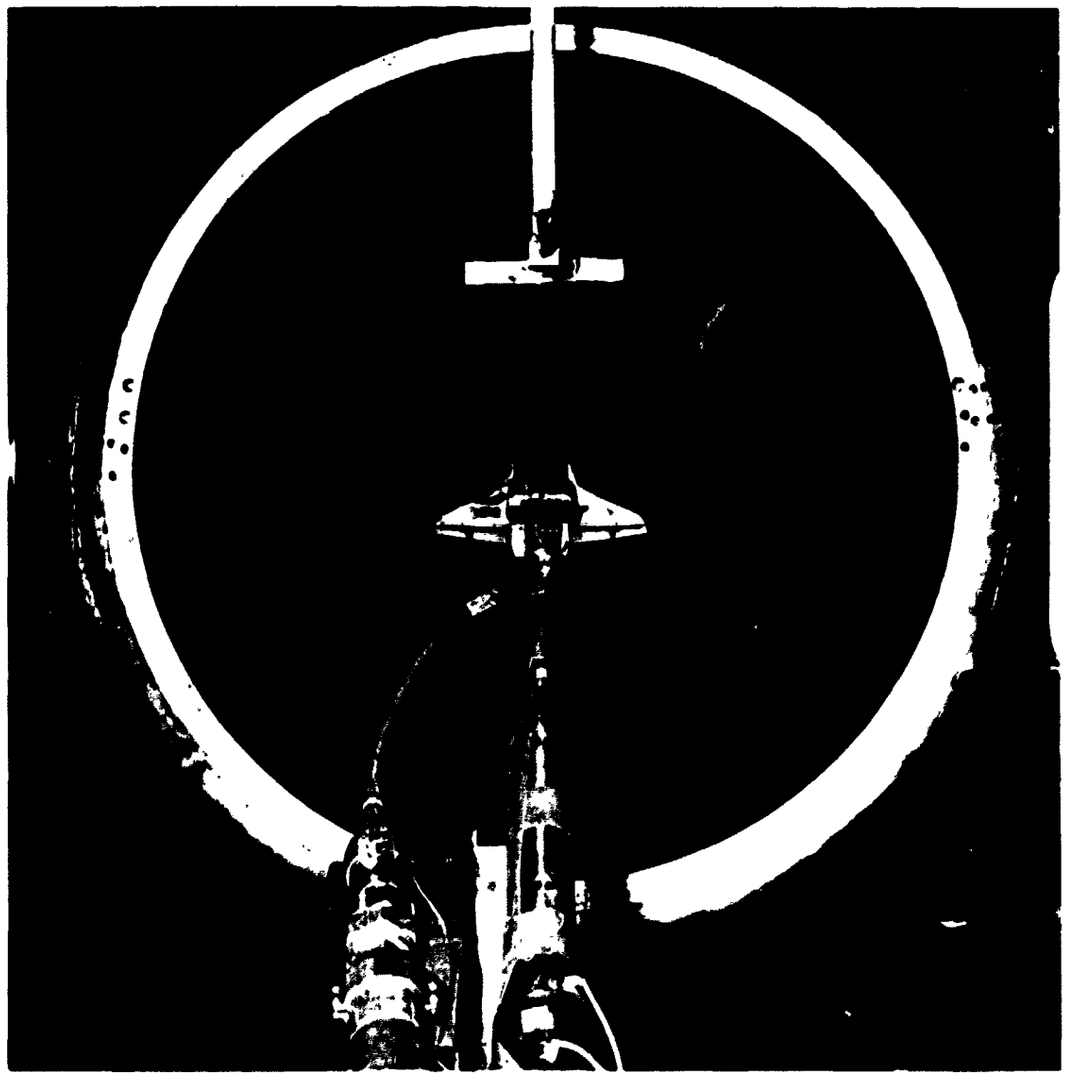

. View looking upstream from RCS plenum tank, showing Valcor valve on separate bracket and flex hose from valve to model plenum.

Figure 3. Model Photographs - (Concluded)

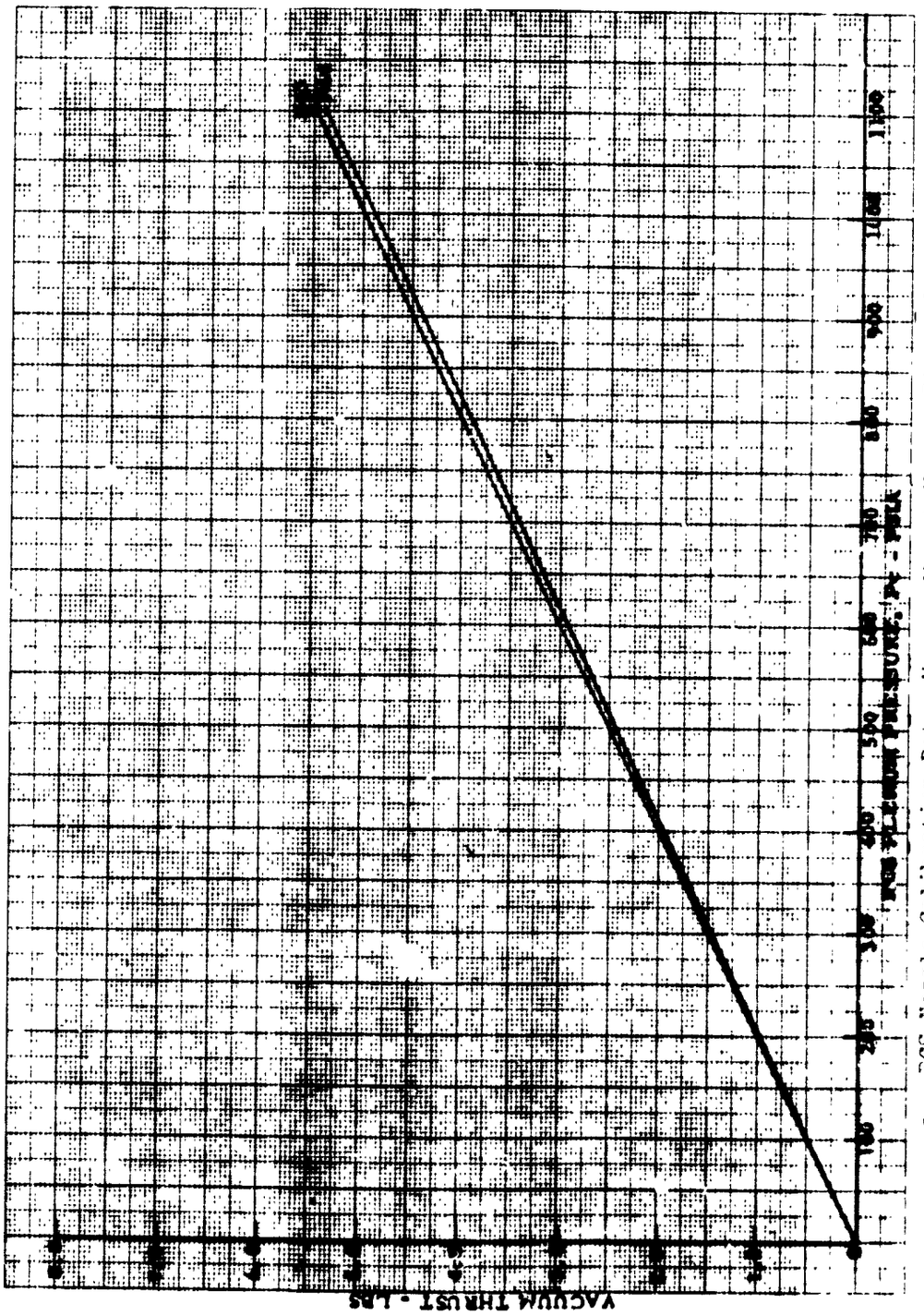

e. RCS Nozzle Calibration Data--Vacuum Thrust Versus Plenum Pressure

Figure 4. Calibration Plots

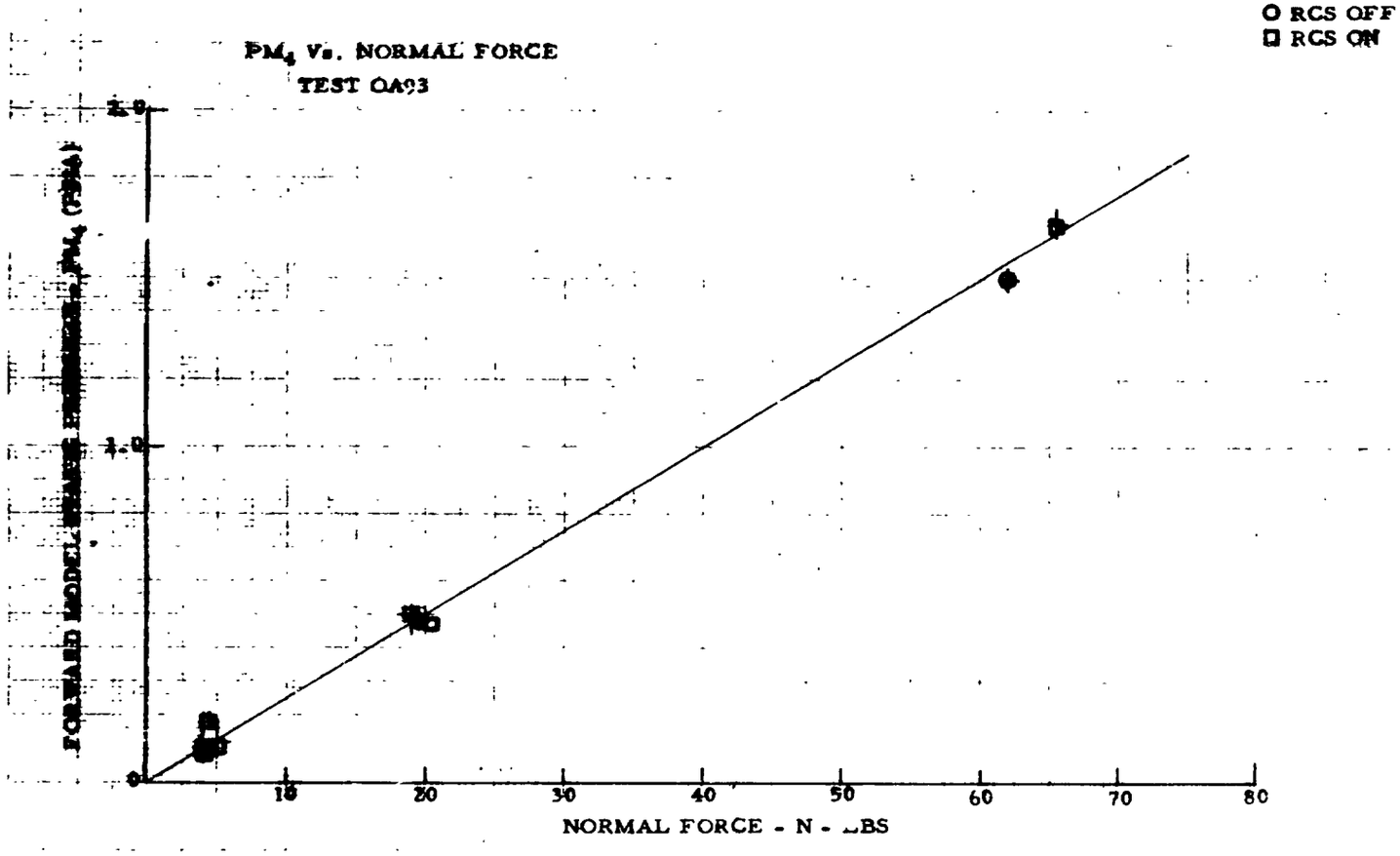

b. Normal Force Vs. Forward Static Pressure for Model 51-O
Figure 4. Calibration Plots - (Cont'd)

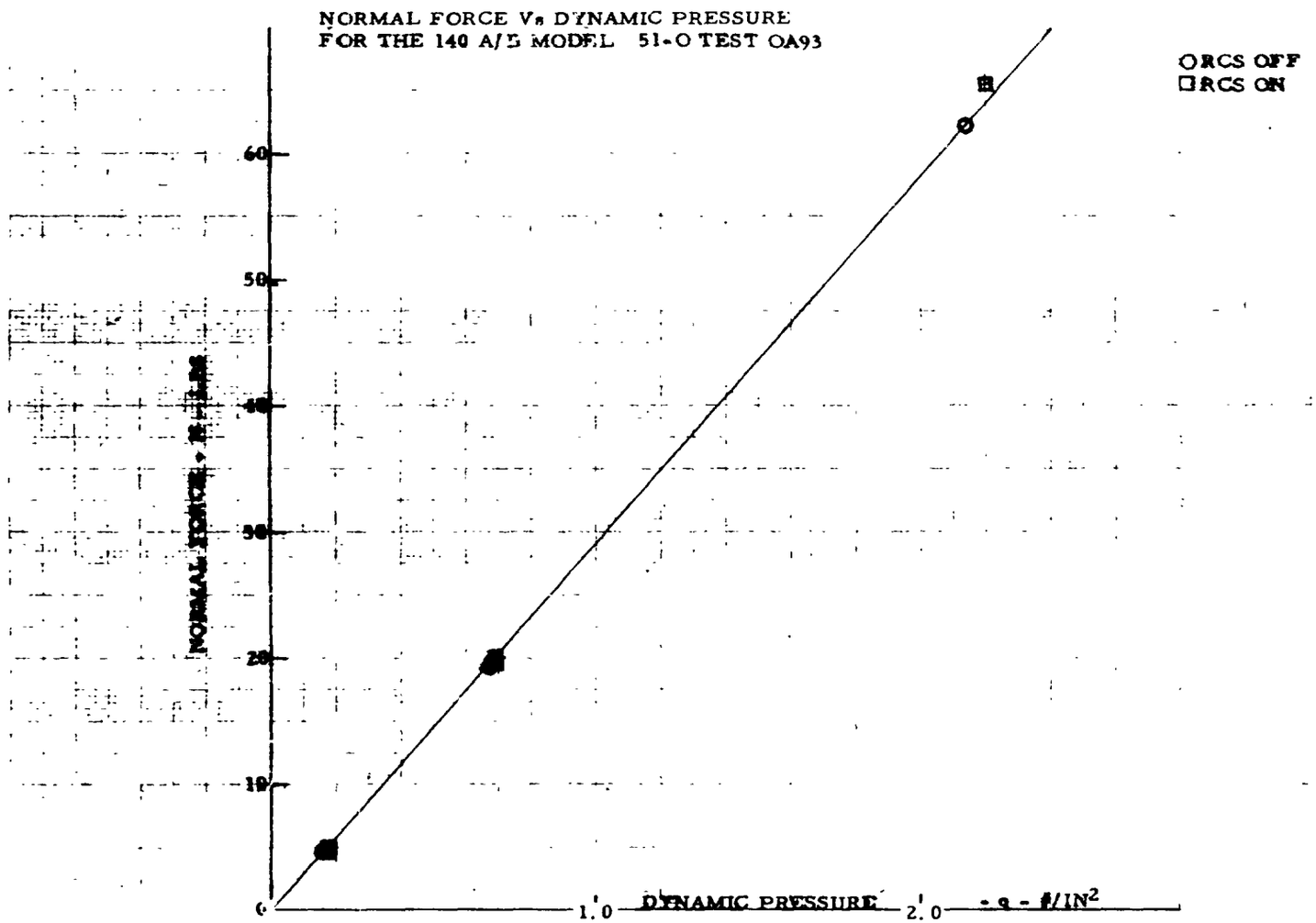

c. Normal Force Vs. Estimated Dynamic Pressure for Model 51-O

Figure 4. Calibration Plots - (Cont'd)

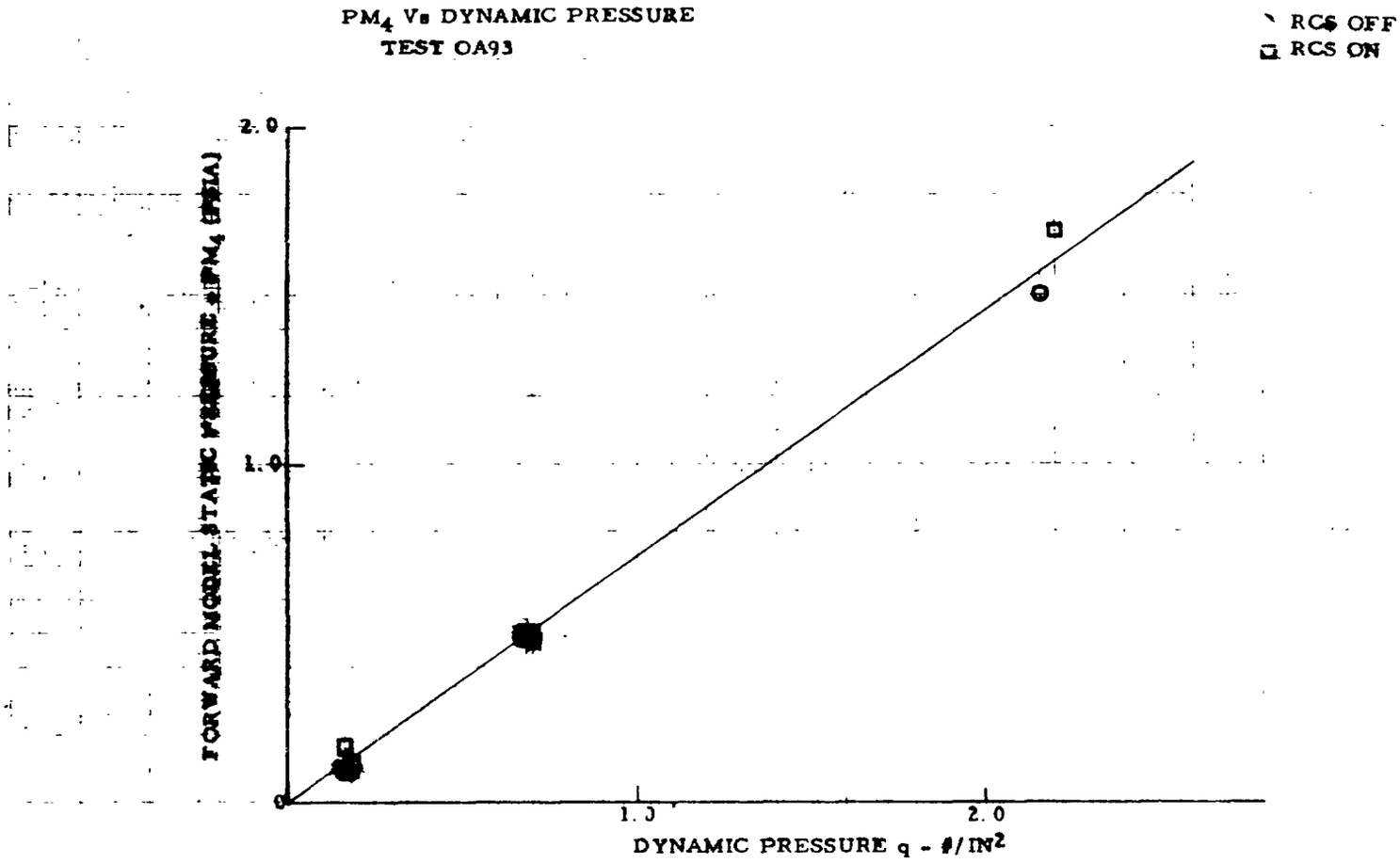

d. Forward Model Static Pressure Vs. Estimated Dynamic Pressure for Model 51-O

Figure 4. - (Concluded)

[illegible], α [illegible]°, Test Condition 4, RCS off
Figure [illegible]. Schlieren Photographs

[illegible], α [illegible]°, Test Condition 4, L/H Pitch Down Jet
Figure 5. [illegible] Schlieren Photographs - (Cont'd)

c. Run 5, $\alpha = 20^{\circ}$, Test Condition 4, L/H Pitch Down Jet.
Figure 5. Schlieren Photographs - (Cont'd)

d. Run 6, $\alpha = 30^{\circ}$, Test Condition 2, RCS off.
Figure 5. Schlieren Photographs - (Cont'd)

e. Run 7, α=30°, Test Conditon 4, R/H Pitch Up Jet
Figure 5. Schlieren Photographs - (Cont'd)

f. Run 8, $\alpha = 30^{\circ}$, Test Condition ?, R/H Pitch Up Jet.
Figure 5. Schlieren Photographs - (Cont'd)

g. Run 9, $\alpha = 30^{\circ}$, Test Condition 2, L/H Pitch Down Jet
Figure 5. Schlieren Photographs - (Cont'd)

h. Run 10, $\alpha = 30^{\circ}$ Test Condition 1, RCS off
Figure 5. Schlieren Photographs - (Cont'd)

i. Run 11, $\alpha = 30^{\circ}$, Test Condition 1, RCS off.

Figure 5. Schlieren Photographs - (Cont'd)

J. Run 12, $\alpha = 30^{\circ}$, Test Condition 1, RCS off.
Figure 5. Schlieren Photographs - (Cont'd)

k. Run 13, α=30°, Test Condition 1, L/H Pitch Down Jet

Figure 5. Schlieren Photographs - (Cont'd)

1. Run 14, $\alpha = 30^{\circ}$, Test Condition C, L/F Pitch Down Jet.
Figure 5. Schlieren Photographs - (Cont'd)

C-2

m. Run 15, $\alpha = 30^{\circ}$, Test Condition 2, RCS off
Figure 5. Schlieren Photographs - (Cont'd)

Direct Impingement Run 102, RCS L/H Pitch Down Jet
Figure 5. Schlieren Photographs - (Cont'd)

o. Direct Impingement Run 107, RCS R/H Pitch Up Jet.
Figure 5. Schlieren Photographs - (Concluded)

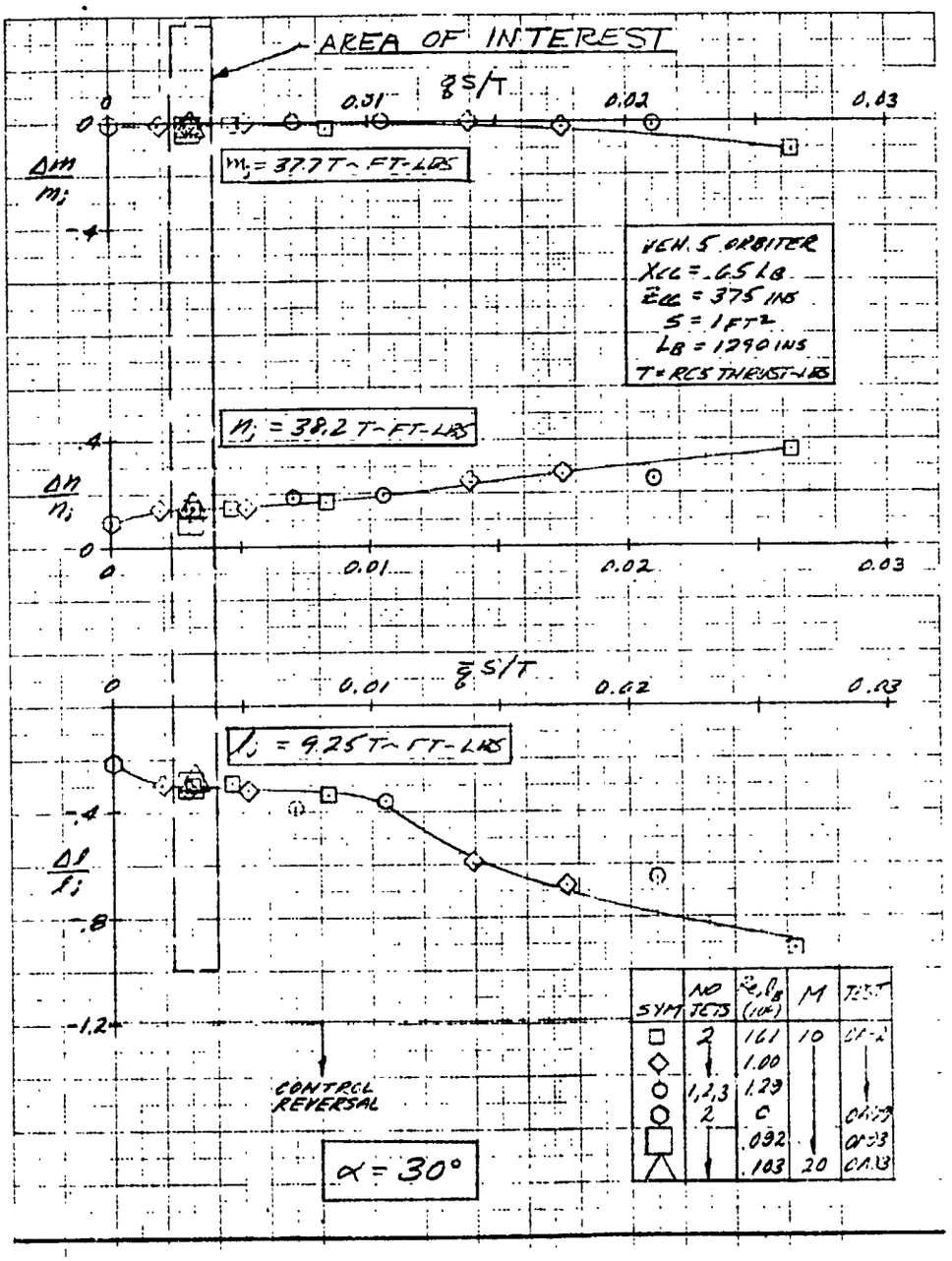

Figure 6. Mach No. and Reynolds No. effect on right hand up-firing jet/aero moment interaction.

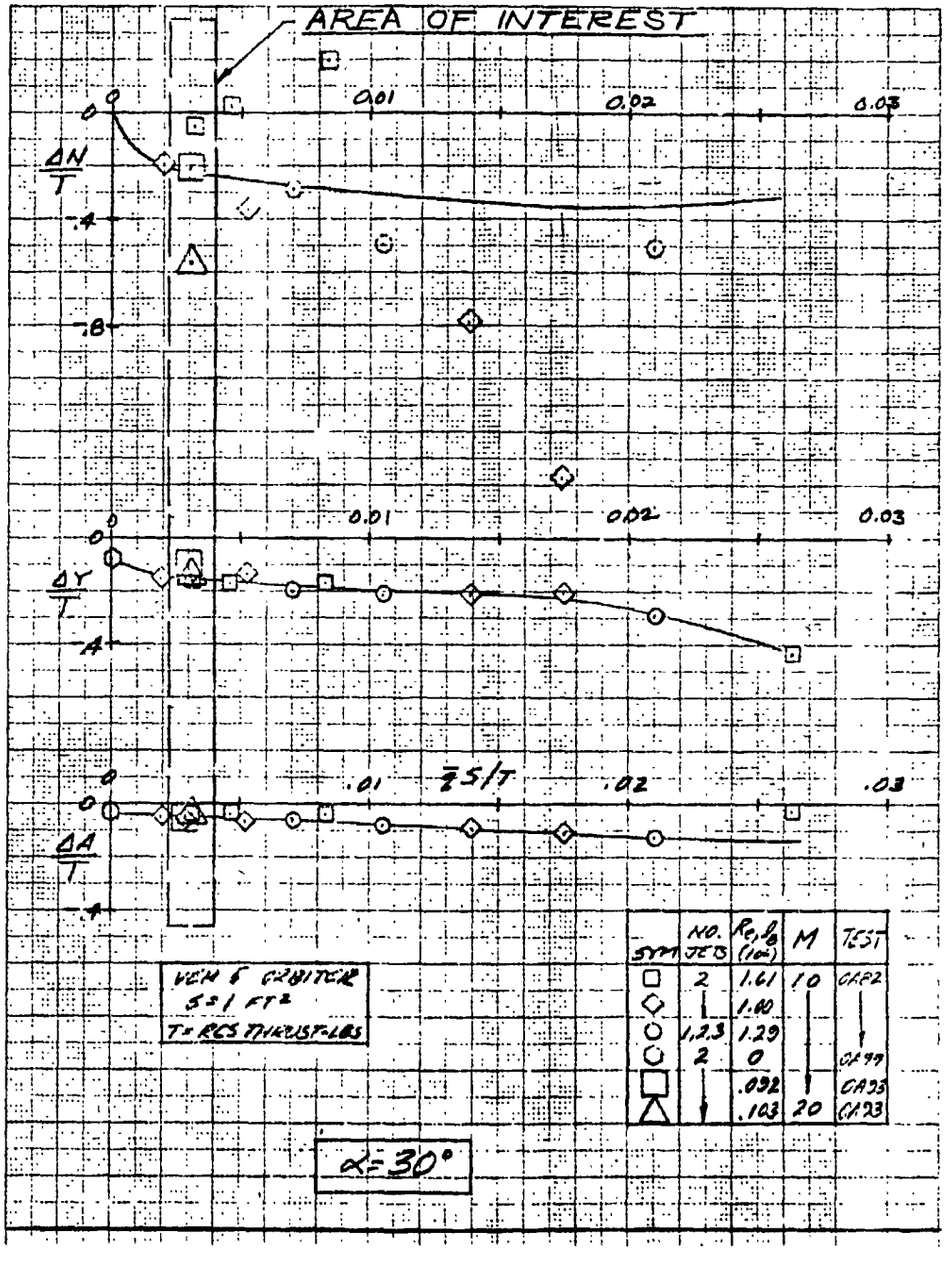

Figure 7. Mach No. and Reynolds No. effect on right hand up-firing jet/aero force interaction.

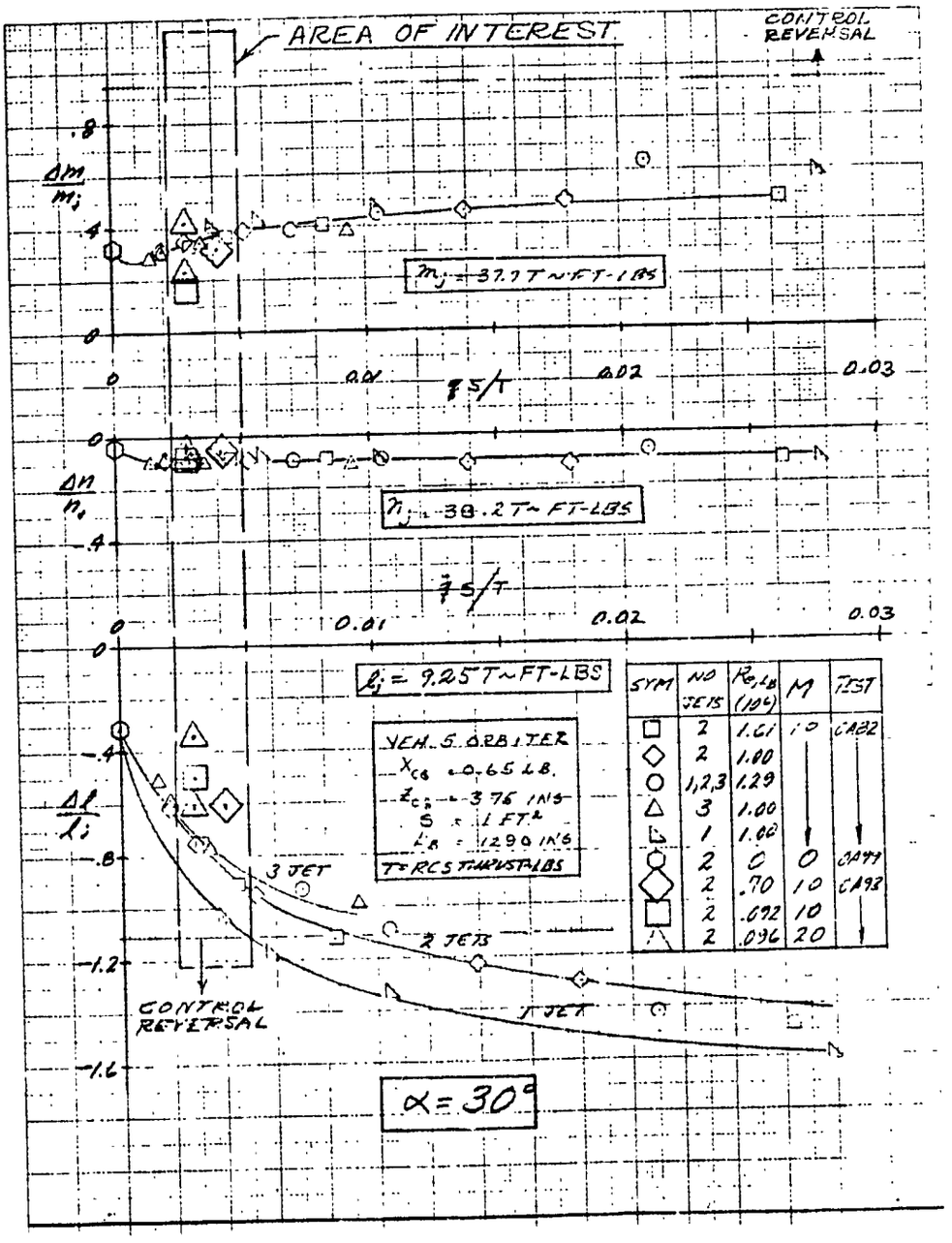

Figure 8. Mach No. and Reynolds No. effect on left hand down-firing jet/aero moment interaction.

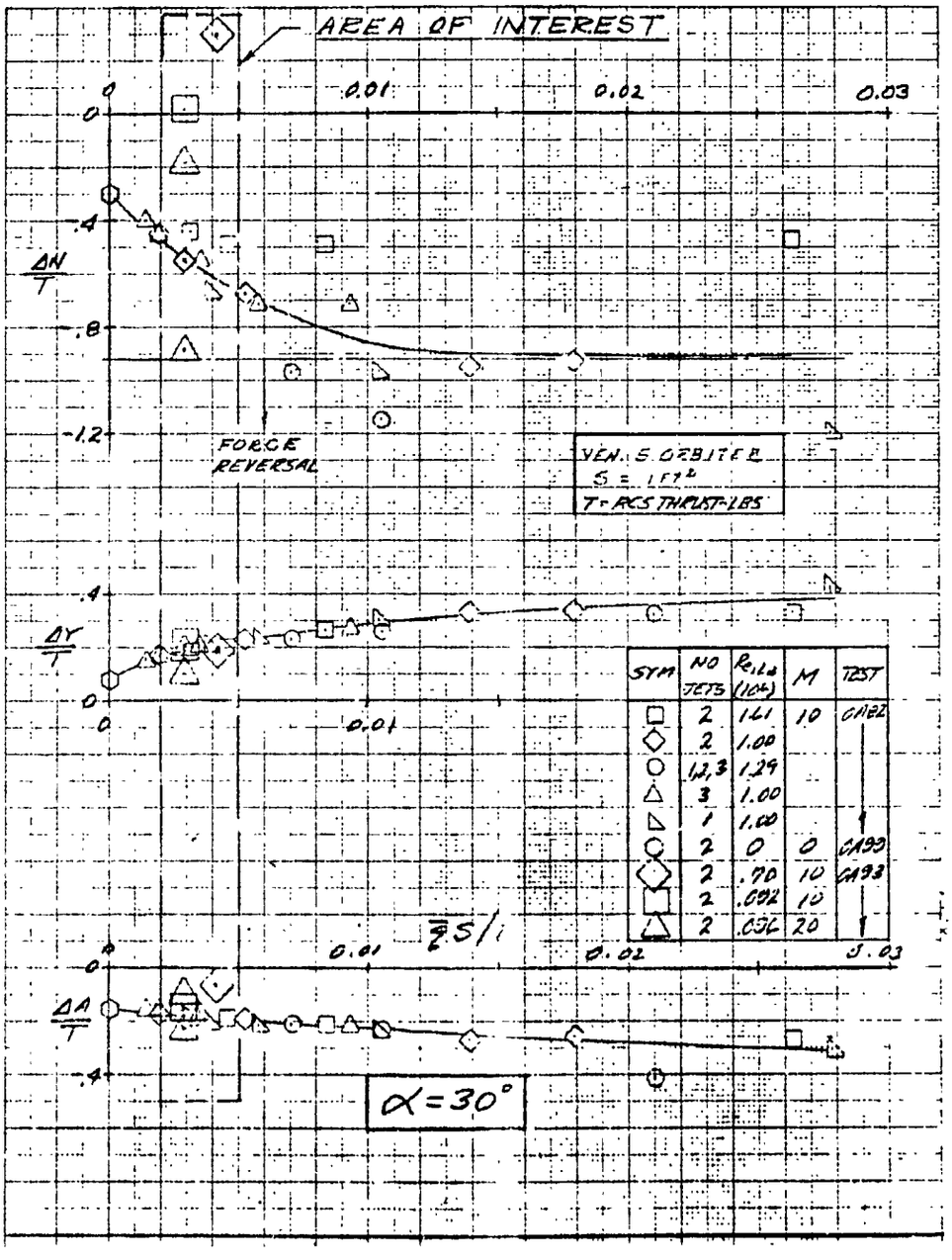

Figure 9. Mach No. and Reynolds No. Effect on Left-hand Down-firing Jet/Aero Force Interaction

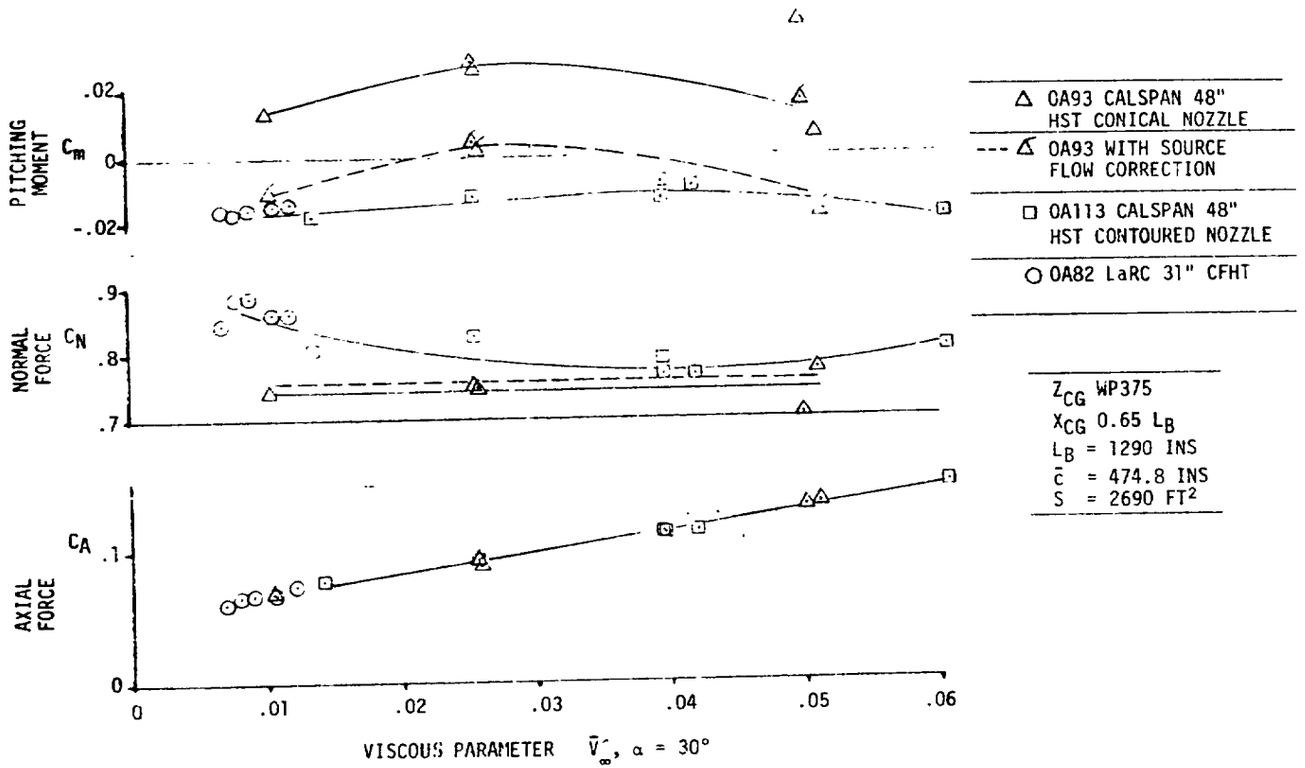

Figure 10. FCS-off Longitudinal Aero Data Vs. Viscous Parameter, $\bar{V}'_\infty$

APPENDIX
TABULATED SOURCE DATA

OA93 B26C9E26F7M15N16R5V8W116 RCS OFF (RU1001)

REFERENCE DATA

SREF = 2690.0000 SQ.FT. XMRP = 1076.7000 IN. XO
LREF = 474.8000 INCHES YMRP = .0000 IN. YO
BREF = 936.7000 INCHES ZMRP = 375.0000 IN. ZO
SCALE = .0100

PARAMETRIC DATA

BETA = .000 ELEVON = .000
BDFLAP = .000 SPDBRK = .000

RUN NO. 6/ 0 RN/L = .08

MACH	ALPHA	CN	CA	CLM	CY	CYN	CBL	PM1	PM2	PM3	PM4
9.635	30.000	.74930	.08886	.02638	-.00237	-.00053	-.00056	.29190	.44950	.35640	.48150

RUN NO. 12/ 0 RN/L = .65

MACH	ALPHA	CN	CA	CLM	CY	CYN	CBL	PM1	PM2	PM3	PM4
10.460	30.000	.74270	.06760	.01342	-.00131	-.00046	-.00061	.88420	1.45600	[illegible]	1.50700

RUN NO. 3/ 0 RN/L = .09

MACH	ALPHA	CN	CA	CLM	CY	CYN	CBL	PM1	PM2	PM3	PM4
19.570	30.000	.77230	.13480	.00636	-.00655	.00002	-.00195	.07549	.10470	[illegible]	.09039

OA93 B26C9E26F7M15N16R5V8W116 RCS OFF (SU1001)

REFERENCE DATA

SREF = 2690.0000 SQ.FT. XMRP = 1076.7000 IN. XO
LREF = 474.8000 INCHES YMRP = .0000 IN. YO
BREF = 936.7000 INCHES ZMRP = 375.0000 IN. ZO
SCALE = .0100

PARAMETRIC DATA

BETA = .000 ELEVON = .000
BDFLAP = .000 SPDBRK = .000

RUN NO. 5/ 0 RN/L = .08

MACH	ALPHA	VBAR	VLBAR	T∞	REFTL	SQRTC∞	PITOT	P(TS)	H(W)	T(W)	C(CP)
9.635	30.000	.02495	.02599	2017.00000	.03829	.76930	1.25400	.00002	3.17100	528.00000	-.01534

RUN NO. 12/ 0 RN/L = .65

MACH	ALPHA	VBAR	VLBAR	T∞	REFTL	SQRTC∞	PITOT	P(TS)	H(W)	T(W)	C(CP)
10.460	30.000	.01034	.01054	1297.00000	03700	.82500	4.02000	.00006	3.15900	526.00000	-.01230

RUN NO. 3/ 0 RN/L = .09

MACH	ALPHA	VBAR	VLBAR	T∞	REFTL	SQRTC∞	PITOT	P(TS)	H(W)	T(W)	C(CP)
19.570	30.000	.05243	.05121	1796.00000	.03363	.81950	.29640	.00006	3.15900	526.00000	-.00041

OA93 B26C9E26F7M15N16R5V8W116 RCS OFF (TU1001)

REFERENCE DATA

SREF = 2690.0000 SQ.FT. XMRP = 1076.7000 IN. XO
LREF = 474.8000 INCHES YMRP = .0000 IN. YO
BREF = 936.7000 INCHES ZMRP = 375.0000 IN. ZO
SCALE = .0100

PARAMETRIC DATA

BETA = .000 ELEVON = .000
BDFLAP = .000 SPDBRK = .000

RUN NO. 6/ 0 RN/L = .08

MACH	ALPHA	M(I)	P(O)	H(O)	T(O)	U	T	P	Q(PSI)	RHO	MU
9.635	30.000	5.28400	607.60000	40.03000	5380.00000	8705.00000	339.40000	.01024	.66630	2.53300	26.84000

RUN NO. 12/ 0 RN/L = .65

MACH	ALPHA	M(I)	P(O)	H(O)	T(O)	U	T	P	Q(PSI)	RHO	MU
10.460	30.000	3.94800	2012.00000	23.60000	3488.00000	6711.00000	171.00000	.02815	2.15900	13.81000	14.29000

RUN NO. 3/ 0 RN/L = .09

MACH	ALPHA	M(I)	P(O)	H(O)	T(O)	U	T	P	Q(PSI)	RHO	MU
19.570	30.000	4.90700	3700.00000	35.01300	4873.00000	8302.00000	74.80000	.00059	.15790	.65980	6.29000

OA93 B26C9E26F7M15N16R5V8W116 RCS OFF (RU1002)

REFERENCE DATA

SREF = 2690.0000 SQ.FT. XMRP = 1076.7000 IN. XO
LREF = 474.8000 INCHES YMRP = .0000 IN. YO
BREF = 936.7000 INCHES ZMRP = 375.0000 IN. ZO
SCALE = .0100

PARAMETRIC DATA

BETA = .000 ELEVON = .000
BDFLAP = .000 SPDBRK = .000

RUN NO. 2/ 0 RN/L = .09

MACH	ALPHA	CN	CA	CLM	CY	CYN	CBL	PM1	PM2	PM3	PM4
19.510	30.000	.70300	.13200	.04113	-.00628	.00458	-.00743	.08359	.11700	.08670	.09744

OA93 TABULATED SOURCE DATA

OA93 B26C9E26F7M15N16R5V8W116 RCS OFF (SU1002)

REFERENCE DATA

SREF = 2690.0000 SQ.FT. XMRP = 1076.7000 IN. XO
LREF = 474.8000 INCHES YMRP = .0000 IN. YO
BREF = 936.7000 INCHES ZMRP = 375.0000 IN. ZO
SCALE = .0100

PARAMETRIC DATA

BETA = .000 ELEVON = .000
BDFLAP = .000 SPDBRK = .000

RUN NO. 2/ 0 RN/L = .09

MACH	ALPHA	VBAR	VLBAR	T∞	REFTL	SQRTC∞	PITCT	P(TS)	H(W)	T(W)	C(CP)
19.510	30.000	.05111	.05013	1838.00000	.03626	.81280	.31930	.00006	3.16500	527.00000	-.00018

OA93 B26C9E26F7M15N16R5V8W116 RCS OFF (TU1002)

REFERENCE DATA

SREF = 2690.0000 SQ.FT. XMRP = 1076.7000 IN. XO
LREF = 474.8000 INCHES YMRP = .0000 IN. YO
BREF = 936.7000 INCHES ZMRP = 375.0000 IN. ZO
SCALE = .0100

PARAMETRIC DATA

BETA = .000 ELEVON = .000
BDFLAP = .000 SPDBRK = .000

RUN NO. 2/ 0 RN/L = .09

MACH	ALPHA	M(∞)	P(O)	H(O)	T(O)	U	T	P	Q(PSI)	RHO	MU
19.510	30.000	4.96800	3989.00000	35.94900	4981.00000	8412.00000	77.29000	.00064	.17000	.69200	6.50000

OA93 B26C9E26F7M15N16R5V8W116 RCS BLOCKS OFF (RU1003)

REFERENCE DATA

SREF = 2690.0000 SQ.FT. XMRP = 1076.7000 IN. XO
LREF = 474.8000 INCHES YMRP = .0000 IN. YO
BREF = 936.7000 INCHES ZMRP = 375.0000 IN. ZO
SCALE = .0100

PARAMETRIC DATA

BETA = .000 ELEVON = .000
BDFLAP = .000 SPDBRK = .000

RUN NO. 15/ 0 RN/L = .08

MACH	ALPHA	CN	CA	CLM	CY	CYN	CBL	PM1	PM2	PM3	PM4
9.620	29.970	.75010	.09097	.02929	-.00356	-.00032	-.00074	.30110	.44650	.35770	.46640

OA93 B26C9E26F7M15N16R5V8W116 RCS BLOCKS OFF (SU1003)

REFERENCE DATA

SREF = 2690.0000 SQ.FT. XMRP = 1076.7000 IN. XO
LREF = 474.8000 INCHES YMRP = .0000 IN. YO
BREF = 936.7000 INCHES ZMRP = 375.0000 IN. ZO
SCALE = .0100

PARAMETRIC DATA

BETA = .000 ELEVON = .000
BDFLAP = .000 SPDBRK = .000

RUN NO. 15/ 0 RN/L = .08

MACH	ALPHA	VBAR	VLBAR	T*	RETTL	SQRTC*	PITOT	P(TS)	H(W)	T(W)	C(CP)
9.620	29.970	.02475	.02577	2005.00000	.08965	.77020	1.26600	.00014	3.16500	527.00000	-.01668

OA93 B26C9E26F7M15N16R5V8W116 RCS BLOCKS OFF (TU1003)

REFERENCE DATA

SREF = 2690.0000 SQ.FT. XMRP = 1076.7000 IN. XO
LREF = 474.8000 INCHES YMRP = .0000 IN. YO
BREF = 936.7000 INCHES ZMRP = 375.0000 IN. ZO
SCALE = .0100

PARAMETRIC DATA

BETA = .000 ELEVON = .000
BDFLAP = .000 SPDBRK = .000

RUN NO. 15/ 0 RN/L = .08

MACH	ALPHA	M(I)	P(O)	H(O)	T(O)	U	T	P	Q(PSI)	RHO	MU
9.620	29.970	5.27700	605.70000	39.78000	5353.00000	8677.00000	338.30000	.01037	.67260	2.57300	26.77000

OA93 B26C9E26F7M15N16R5V8W116 N42 RCS ON (RU1004)

REFERENCE DATA

SREF = 2690.0000 SQ.FT. XMRP = 1076.7000 IN. XO
LREF = 474.8000 INCHES YMRP = .0000 IN. YO
BREF = 936.7000 INCHES ZMRP = 375.0000 IN. ZO
SCALE = .0100

PARAMETRIC DATA

BETA = .000 ELEVON = .000
BDFLAP = .000 SPDBRK = .000

RUN NO. 14/ 0 RN/L = .09

MACH	ALPHA	CN	CA	CLM	CY	CYN	CBL	PM1	PM2	PM3	PM4
9.559	29.980	.75290	.07115	.04884	.02315	-.00358	-.00901	.31520	.47480	.38040	.51320

RUN NO. 13/ 0 RN/L = .65

MACH	ALPHA	CN	CA	CLM	CY	CYN	CBL	PM1	PM2	PM3	PM4
10.530	29.980	.76990	.06260	.04119	.01565	-.00320	-.00713	1.02700	.00000	1.32500	1.67400

RUN NO. 5/ 0 RN/L = .09

MACH	ALPHA	CN	CA	CLM	CY	CYN	CBL	PM1	PM2	PM3	PM4
19.320	30.000	.65760	.10490	.05884	.01830	-.00280	-.01136	.07317	.11090	.08743	.11470

OA93 B26C9E26F7M15N16R5V8W116 N42 RCS ON (SU1004)

REFERENCE DATA

SREF = 2690.0000 SQ.FT. XMRP = 1076.7000 IN. XO
LREF = 474.8000 INCHES YMRP = .0000 IN. YO
BREF = 936.7000 INCHES ZMRP = 375.0000 IN. ZO
SCALE = .0100

PARAMETRIC DATA

BETA = .000 ELEVON = .000
BDFLAP = .000 SPDBRK = .000

RUN NO. 14/ 0 RN/L = .09

MACH	ALPHA	VBAR	VLBAR	T*	REFTL	SQRTC*	PITOT	P(TS)	H(W)	T(W)	C(CP)
9.559	29.980	.02435	.02536	2006.00000	.09155	.77070	1.30600	.00014	3.16500	527.00000	-.00412

RUN NO. 13/ 0 RN/L = .65

MACH	ALPHA	VBAR	VLBAR	T*	REFTL	SQRTC*	PITOT	P(TS)	H(W)	T(W)	C(CP)
10.530	29.980	.01036	.01057	1317.00000	.69870	.82250	4.09800	.00006	3.16500	527.00000	-.00306

RUN NO. 5/ 0 RN/L = .09

MACH	ALPHA	VBAR	VLBAR	T*	REFTL	SQRTC*	PITOT	P(TS)	H(W)	T(W)	C(CP)
19.320	30.000	.05111	.05011	1809.00000	.09502	.81530	.31230	.00004	3.16500	527.00000	.00298

OA93 B26C9E26F7M15N16R5V8W116 N42 RCS ON (TU1004)

REFERENCE DATA

SREF = 2690.0000 SQ.FT. XMRP = 1076.7000 IN. XO
LREF = 474.8000 INCHES YMRP = .0000 IN. YO
BREF = 936.7000 INCHES ZMRP = 375.0000 IN. ZO
SCALE = .0100

PARAMETRIC DATA

BETA = .000 ELEVON = .000
BDFLAP = .000 SPDBRK = .000

RUN NO. 14/ 0 RN/L = .09

MACH	ALPHA	M(I)	P(O)	H(O)	T(O)	U	T	P	Q(PSI)	RHO	MU
9.559	29.980	5.27700	606.60000	39.78000	5353.00000	8674.00000	342.40000	.01083	.69370	2.65500	27.05000

RUN NO. 13/ 0 RN/L = .65

MACH	ALPHA	M(I)	P(O)	H(O)	T(O)	U	T	P	Q(PSI)	RHO	MU
10.530	29.980	3.98400	2131.00000	24.07000	3547.00000	6778.00000	172.20000	.02830	2.20000	13.80000	14.39000

RUN NO. 5/ 0 RN/L = .09

MACH	ALPHA	M(I)	P(O)	H(O)	T(O)	U	T	P	Q(PSI)	RHO	MU
19.320	30.000	4.91800	3682.00000	35.29000	4906.00000	8334.00000	77.35000	.00064	.16640	.68980	6.50400

OA93 TABULATED SOURCE DATA

OA93 B26C9E26F7M15N16R5V8W116 N42 RCS ON (RU1005)

REFERENCE DATA

SREF =	2690.0000 SQ.FT.	XMRP =	1076.7000 IN.	XO	
LREF =	474.8000 INCHES	YMRP =	.0000 IN.	YO	
BREF =	936.7000 INCHES	ZMRP =	375.0000 IN.	ZO	
SCALE =	.0100				

PARAMETRIC DATA

BETA =	.000	ELEVON =	.000
BDFLAP =	.000	SPDBRK =	.000

RUN NO. 47 0 RN/L = .09

MACH	ALPHA	CN	CA	CLM	CY	CYN	CBL	PM1	PM2	PM3	PM4
19.580	30.000	.74900	.12200	.03526	.00636	-.00498	-.00724	.08038	.11830	.10090	.17310

OA93 B26C9E26F7M15N16R5V8W116 N42 RCS ON (SU1005)

REFERENCE DATA

SREF =	2690.0000 SQ.FT.	XMRP =	1076.7000 IN.	XO	
LREF =	474.8000 INCHES	YMRP =	.0000 IN.	YO	
BREF =	936.7000 INCHES	ZMRP =	375.0000 IN.	ZO	
SCALE =	.0100				

PARAMETRIC DATA

BETA =	.000	ELEVON =	.000
BDFLAP =	.000	SPDBRK =	.000

RUN NO. 47 0 RN/L = .09

MACH	ALPHA	VBAR	VLBAR	T*	REFTL	SQRTC*	PITOT	P(TS)	H(W)	T(W)	C(CP)
19.580	30.000	.05136	.05030	1831.00000	.09641	.81440	.31540	.00004	3.17100	528.00000	.00015

OA93 B26C3E26F7M15N16R5V8W116 N42 RCS ON (TU1005)

REFERENCE DATA

SREF =	2690.0000 SQ.FT.	XMRP =	1076.7000 IN.	XO	
LREF =	474.8000 INCHES	YMRP =	.0000 IN.	YO	
BREF =	935.7000 INCHES	ZMRP =	375.0000 IN.	ZO	
SCALE =	.0100				

PARAMETRIC DATA

BETA =	.000	ELEVON =	.000
BDFLAP =	.000	SPDBRK =	.000

RUN NO. 47 0 RN/L = .09

MACH	ALPHA	M(I)	P(O)	H(O)	T(C)	U	T	P	Q(PSI)	RHO	MU
19.580	30.000	4.94700	4000.00000	35.79000	4965.00000	8394.00000	76.41000	.0006[illegible]	.16800	.68650	6.42600

OA93 B26C9E26F7M15N16R5V8W116 N44 RCS ON (RU1006)

REFERENCE DATA

SREF =	2690.0000 SQ.FT.	XMRP =	1076.7000 IN. XO		
LREF =	474.8000 INCHES	YMRP =	.0000 IN. YO		
BREF =	936.7000 INCHES	ZMRP =	375.0000 IN. ZO		
SCALE =	.0100				

PARAMETRIC DATA

BETA =	.000	ELEVON =	.000
BDFLAP =	.000	SPDBRK =	.000

RUN NO. 8/ 0 RN/L = .09

MACH	ALPHA	CN	CA	CLM	CY	CYN	CBL	PM1	PM2	PM3	PM4
9.590	29.980	.72400	.08447	.02601	-.01764	.00566	-.00483	.32590	.46200	.37400	.50220

RUN NO. 7/ 0 RN/L = .10

MACH	ALPHA	CN	CA	CLM	CY	CYN	CBL	PM1	PM2	PM3	PM4
19.160	30.000	.70390	.12910	.00380	-.02312	.00862	-.00596	.08804	.12110	.09288	.12320

OA93 B26C9E26F7M15N16R5V8W116 N44 RCS ON (SU1006)

REFERENCE DATA

SREF =	2690.0000 SQ.FT.	XMRP =	1076.7000 IN. XO		
LREF =	474.8000 INCHES	YMRP =	.0000 IN. YO		
BREF =	936.7000 INCHES	ZMRP =	375.0000 IN. ZO		
SCALE =	.0100				

PARAMETRIC DATA

BETA =	.000	ELEVON =	.000
BDFLAP =	.000	SPDBRK =	.000

RUN NO. 8/ 0 RN/L = .09

MACH	ALPHA	VBAR	VLBAR	T°	REFTL	SQRTC°	PITOT	P(TS)	H(W)	T(W)	C(CP)
9.590	29.980	.02438	.02539	2013.00000	.09179	.77010	1.31100	.00004	3.15300	525.00000	-.01546

RUN NO. 7/ 0 RN/L = .10

MACH	ALPHA	VBAR	VLBAR	T°	REFTL	SQRTC°	PITOT	P(TS)	H(W)	T(W)	C(CP)
19.160	30.000	.04855	.04775	1824.00000	.10260	.81160	.34840	.00002	3.14100	523.00000	-.00378

OA93 B26C9E26F7M15N16R5V8W116 N44 RCS ON (TU1006)

REFERENCE DATA

SREF = 2690.0000 SQ.FT. XMRP = 1076.7000 IN. XO
LREF = 474.8000 INCHES YMRP = .0000 IN. YO
BREF = 936.7000 INCHES ZMRP = 375.0000 IN. ZO
SCALE = .0100

PARAMETRIC DATA

BETA = .000 ELEVON = .000
BDFLAP = .000 SPDBRK = .000

RUN NO. 8/ 0 RN/L = .09

MACH	ALPHA	M(I)	P(O)	H(O)	T(O)	U	T	P	Q(PSI)	RHO	MU
9.590	29.980	5.31200	620.30000	39.97000	5367.00000	8696.00000	341.90000	.01081	.69630	2.65200	27.01000

RUN NO. 7/ 0 RN/L = .10

MACH	ALPHA	M(I)	P(O)	H(O)	T(O)	U	T	P	Q(PSI)	RHO	MU
19.160	30.000	4.98700	3964.00000	35.66000	4943.00000	8377.00000	79.48000	.00072	.18560	.76150	6.68500

OA93 B26C9E26F7M15N16R5V8W116 N42 RCS ON (RU1007) (30 OCT 75)

REFERENCE DATA

SREF = 2690.0000 SQ.FT. XMRP = 1076.7000 IN. XO
LREF = 474.8000 INCHES YMRP = .0000 IN. YO
BREF = 936.7000 INCHES ZMRP = 375.0000 IN. ZO
SCALE = .0100

PARAMETRIC DATA

BETA = .000 ELEVON = .000
BDFLAP = .000 SPDBRK = .000

RUN NO. 102/ 0 RN/L = .00 GRADIENT INTERVAL = -5.00/ 5.00

MACH	ALPHA	CN	CA	CLM	CY	CYN	CBL	C(CP)
.000	30.000	-.00732	-.00334	.00716	.00230	-.00087	-.00100	.00030
	GRADIENT	.00000	.00000	.00000	.00000	.00000	.00000	.00000

OA93 B26C9E26F7M15N16R5V8W116 N42 RCS ON (RU1008) (30 OCT 75)

REFERENCE DATA

SREF = 2690.0000 SQ.FT. XMRP = 1076.7000 IN. XO
LREF = 474.8000 INCHES YMRP = .0000 IN. YO
BREF = 936.7000 INCHES ZMRP = 375.0000 IN. ZO
SCALE = .0100

PARAMETRIC DATA

BETA = .000 ELEVON = .000
BDFLAP = .000 SPDBRK = .000

RUN NO. 105/ 0 RN/L = .00 GRADIENT INTERVAL = -5.00/ 5.00

MACH	ALPHA	CN	CA	CLM	CY	CYN	CBL	C(CP)
.000	30.000	-.00355	-.00369	.00703	.00232	-.00074	-.00085	.00040
	GRADIENT	.00000	.00000	.00000	.00000	.00000	.00000	.00000

0A93 B26C9E26F7M15N16R5V8W116 N44 RCS ON (RUI009) (30 OCT 75)

REFERENCE DATA

SREF =	2690.0000 SQ.FT.	XMRP =	1076.7000 IN.	XO	
LREF =	474.8000 INCHES	YMRP =	.0000 IN.	YO	
BREF =	936.7000 INCHES	ZMRP =	375.0000 IN.	ZO	
SCALE =	.0100				

PARAMETRIC DATA

BETA =	.000	ELEVON =	.000
BDFLAP =	.000	SPDBRK =	.000

RUN NO. 107/ 0 RN/L = .00 GRADIENT INTERVAL = -5.00/ 5.00

MACH	ALPHA	CN	CA	CLM	CY	CYN	CBL	C(CP)
.000	30.000	.00021	-.00085	-.00018	-.00197	.00033	-.00097	.00012
	GRADIENT	.00000	.00000	.00000	.00000	.00000	.00000	.00000